Chapter VIII

TRITIUM AND BLANKET

M.A. ABDOU – USA
G. CASINI – EC
F.N. FLAKUS – IAEA
T. HIRAOKA – Japan
T. KOBAYASHI – Japan
B.N. KOLBASOV – USSR
D. LEGER – EC
M. ROGERS – USA
K. TOMABECHI – Japan
G.E. SHATALOV – USSR
T. SUZUKI – Japan
V.G. VASIL'EV – USSR

1. INTRODUCTION

The main objectives of Phase Two A were established to develop the tritium breeding blanket and to evaluate tritium permeation, inventory and contamination in all INTOR systems.

These basic tasks include:

(a) Tritium permeation into coolant:
- evaluate models and experimental data for tritium permeation from plasma to first wall and divertor (limiter) coolant systems;
- assess methods for tritium separation from water;
- calculate the tritium inventory in the components facing the plasma and outgassing during dwell time and after shut-down.

(b) Tritium contamination of reactor environment:
- identify sources of tritium contamination in the reactor environment in normal and accident conditions;
- evaluate pathways and effects of tritium leaks;
- recommend a strategy for air purification and personnel access inside the reactor room.

(c) Tritium-producing blanket design:
- review and up-date data base for solid breeders (Li_2O, $LiAlO_2$, Li_2SiO_3) and for low-reactivity liquid breeder ($Li_{17}Pb_{83}$);
- revise blanket conceptual designs developed during Phase One for these two types of breeder.

(d) Tritium systems study:
- plasma reprocessing system
- blanket processing system
- air detritiation system
- waste processing system.

(e) Safety analyses:
- improve accident scenarios and evaluate their effects on the reactor design and operation;
- evaluate the dose rates to the environment in case of routine and accident conditions;
- assess the problems of waste disposal.

The results of the study undertaken in 1981 and 1982 are presented in this chapter.

2. TRITIUM PERMEATION INTO COOLANT

Tritium permeation into the coolant of the first wall, limiter and divertor was identified as a key issue for fusion devices during the INTOR Phase-One study. There are large uncertainties in key parameters and processes that govern tritium permeation. Some of these uncertainties can be resolved by relatively simple experiments in the near future. Other uncertainties require experiments in an actual fusion environment. The purpose of this work is to evaluate and characterize the tritium permeation issues and identify the key R and D requirements.

2.1. Tritium permeation rate

Tritium permeation through first walls, limiters, or divertors subject to energetic tritium charge-exchange neutral bombardment is a potentially serious problem area for advanced DT reactors operating at elevated temperatures. High concentrations of tritium in the near-surface region can be reached by implantation of the charge-exchange neutral flux combined with a relatively slow recombination of these atoms into molecules at the plasma/first-wall interface. Because of this large concentration of mobile tritium near the inner (plasma) wall surface, a concentration gradient is established, causing tritium to diffuse into the bulk and eventually to the outer wall surface where it can enter the first-wall coolant.

Initial calculations by Wienhold et al. [7] have shown that as much as 16 g of tritium (1.6×10^5 Ci) per day could permeate through a stainless-steel, INTOR-sized vessel operated at a uniform temperature of 600°C and bombarded with $10^{17}\ cm^{-2}\cdot s^{-1}$ flux to the first wall.

Calculations are presented in Section 2.1.3 for a stainless-steel wall and a limiter or divertor plate. The unknown surface conditions prevailing in a reactor result in a large uncertainty as to the magnitude of the recombination processes which, as we have seen above, determine the driving force for permeation. In addition, the lack of neutron damage trapping characteristics severely limits our ability to predict the tritium inventory and time to permeation breakthrough.

2.1.1. Theoretical models and calculations

Calculations were performed by all countries to estimate the tritium permeation and inventory of first wall, limiter and divertor [3–6]. The time-dependent diffusion equation with an implant source and point defect trapping can be solved numerically. The surface boundary condition on the inner (plasma) surface is assumed to be characterized by a recombination constant for an endothermic metal as given by:

$$k_r = \frac{5.25 \times 10^{25}\ (k^{1/2}\cdot atm^{-1}\cdot cm^{-2}\cdot s^{-1})}{C_0^{*2}\sqrt{T}}\ \alpha \exp\left[(E_s - E_D)/kT\right] \qquad (1)$$

where E_D is the activation energy for migration, E_s is the heat of solution and C_0^* is the Sievert's law constant. The factor α is the molecular sticking coefficient; it is taken to be a measure of surface cleanliness. Since α depends on surface composition, presence of oxides, carbon contamination, etc. it cannot be defined uniquely but, instead, must be measured for each particular experimental environment.

In the bulk of the sample, simple diffusion is assumed to occur, with the diffusivity given by:

$$D = D_0 \exp\left(-E_D/kT\right) \qquad (2)$$

In addition, hydrogen is allowed to diffuse because of a thermal gradient (Soret effect). The tritium flux in the bulk is, therefore, given by:

$$J = -D\frac{\partial C}{\partial x} + \frac{CQ^*}{kT^2}\frac{\partial T}{\partial x} \qquad (3)$$

where Q^* is the heat of transport. The diffusion of hydrogen in a thermal gradient has not been studied in detail for many metals. While bcc iron and nickel show a

negative Q^* [9] (i.e. hydrogen diffusion to the hot side), a positive Q^* has been reported for zirconium [10]. The present study uses a constant value of $Q^* = -0.065$ eV for stainless steel, based on data for nickel at $\cong 800$ K [9]. No data are available for beryllium. Deviations from Fickian diffusion due to the hypothesized interaction of hydrogen with mobile point defects [11, 12] are not considered in this study. Trapping to a uniform concentration, C_T, of neutron-damage-produced traps of total detrapping energy, E_T, from zero time is included.

The potentially more complex surface conditions on the coolant-wall interface are approximated by recombination-limited kinetics or a $C = 0$ (diffusion-limited) boundary condition. The existence of oxide layers, as well as the presence of water instead of vacuum, may complicate the situation but few experimental data exist. Hydrogen produced by the radiolytic decomposition of the coolant water may also affect the boundary condition.

The choice of boundary conditions in the permeation and inventory calculations is very important. Several alternatives to the assumption stated previously were investigated. The approach detailed in the Soviet report [6] is worth being explained.

The surface recombination rate is the sum of several values connected with different processes of hydrogen release from the wall. One of them is thermally induced desorption which can be described by boundary conditions in form

$$J = 2KrC^2 \tag{4}$$

The second process is ion-induced desorption for which

$$J = KjC + (1-r)j \tag{5}$$

where j is the incident flux, r the reflection coefficient, and K depends on boundary temperature and conditions. Photoelectron temperature and condition processes are also possible in tokamak operating conditions.

It was shown in Ref. [6] that in the most important cases any boundary condition can be changed to the condition of the first kind, i.e.

$$C(0,t) = C(0) = \text{const} \tag{6}$$

$C(0)$ depends on surface temperature, incident flux, ion energy, etc. and can be estimated from experimental data. In this case, it is possible to achieve, to some approximation, an analytical solution of the diffusion equation in a plate with a linear temperature drop $\Delta T = T_0 - T_1$. The ratio of penetrating fluxes in the cases of constant temperature and linear temperature drop is

$$\frac{q/\Delta t}{q/T_0} \cong \frac{\beta}{e^{\beta}-1} \tag{7}$$

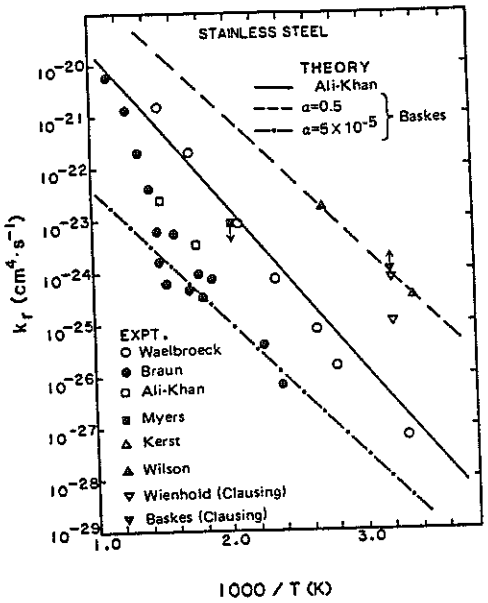

FIG. VIII-1. Comparison of experimental data for k_r of stainless steel and the theory of Baskes [8] for two values of the molecular sticking coefficient, α.

where

$$\beta = \frac{E_D \Delta T}{T_0 - T_1}$$

Analogous expressions were solved for the inventory in the wall and the permeation time. $C(0)$ and its dependence on surface temperature and incident flux (the latter is linear) were calculated from the experimental data.

2.1.2. *Experimental results*

As was mentioned in Section 2.1.1, the molecular sticking coefficient α is a key factor in determining the surface boundary condition. This sticking coefficient depends on surface composition, cleanliness, etc. Values of α from 0.5 (clean surface) to 5×10^{-5} have been reported in the literature [8]. A summary of the experimental data is shown in Fig. VIII-1.

TABLE VIII-1. PARAMETERS USED FOR THREE CASES OF INTOR FIRST WALL AND LIMITER/DIVERTOR

Material parameters		INTOR base case stainless-steel wall	INTOR Case 1: stainless-steel first wall and limiter	INTOR Case 2: Be/Cu limiter/divertor plate Be	Cu
Diffusivity	D_0 ($cm^2 \cdot s^{-1}$)	0.085	0.085	3×10^{-7}	1.1×10^{-2}
	E_d (eV)	0.61	0.61	0.19	0.4
	q^* (eV)	−0.065	−0.065	0	0
Solubility	C_0	7.65×10^{19} atoms·cm^{-3}·$atm^{-1/2}$	9×10^{-4} $atm^{-1/2}$	6.1×10^{-6} $atm^{-1/2}$	1.6×10^{-3} $atm^{-1/2}$
	E_s (eV)	0.091	0.091	0.0	0.37
Trapping	E_T (eV)	No trapping	0.85	1.5	1.0
	C_T (at.fr.)		0.01	0.01	0.01
Surface condition	α_{inner}	$0.5/5 \times 10^{-5}$	5×10^{-3}	0.5	–
	c_{outer}	$10^{-4} < \alpha_0/\alpha_i < 1$	0	–	0
Thickness (cm)		1.34	0.5	1.0	0.15
Area (m^2)		400	400	60	
Operating conditions					
Temperature	T_{inner} (°C)	300	180		467
	$T_{interface}$ (°C)				200
	T_{outer} (°C)	100	100		187
Plasma	ϕ(D-T·cm^{-2}·s^{-1})	3.3×10^{16}	2.5×10^{16}	3×10^{18}	
	E (eV)	200; Maxwellian; cosine angular	200; Maxwellian; cosine angular	675 ; normal incidence	
Duty cycle		0.8^{16}	continuous	continuous	

FIG. VIII-2. Calculated tritium permeation rates for Base Case INTOR first wall under standard operating conditions. Both 'clean' ($\alpha_i = 0.5$) and 'dirty' ($\alpha_i = 5 \times 10^{-5}$) inner-wall surface conditions are considered [25].

Three distinctly different classes of experiments were performed by various countries [3–6]. The largest number of experiments were of the ion bombardment type, followed by glow discharges and a limited number of in-situ tokamak tests. The detailed descriptions and results of these experiments can be found in the national reports.

2.1.3. Calculational results

Several cases for the INTOR first wall and limiter/divertor were investigated [5, 25]. The parameters used for three cases of interest are summarized in Table VIII-1. The first column is the INTOR Base Case 1.34-cm stainless-steel first wall. Figure VIII-2 shows the steady-state permeation rates obtained for the standard INTOR conditions, with the inner surface molecular sticking coefficient equal to 0.5 ('clean' surface) or 5×10^{-5} ('dirty' surface) and the outer surface sticking coefficient a fraction from unity to 10^{-4} of the inner surface value. The highest tritium permeation rate (>0.1 g per day) is obtained for a 'dirty' inner surface ($\alpha_i = 5 \times 10^{-5}$), and relatively high recombination ($\alpha_0/\alpha_i \geq 1$) at the outer surface. As $\alpha_0/\alpha_i \to \infty$, the tritium permeation rate approaches 5.5×10^{-3} g per day for a 'clean' inner surface and 0.55 g per day for a 'dirty' inner surface. In the ideal conditions of a 'clean' inner surface ($\alpha_i = 0.5$) and slow recombination at the coolant side ($\alpha_0/\alpha_i \leq 10^{-4}$), tritium permeation is

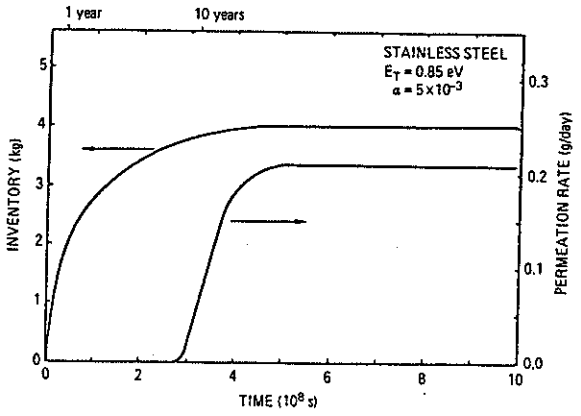

FIG. VIII-3. Calculated tritium permeation rate and inventory for a stainless-steel first wall (INTOR Case 1).

TABLE VIII-2. EFFECTS OF TEMPERATURE ON TRITIUM PERMEATION AND INVENTORY FOR INTOR CASE 1: STAINLESS STEEL

	With trapping (C_t = 0.01; E_t = 0.85 eV)		
Temperature plasma/coolant (°C)	Time to permeation breakthrough[a] (s)	Steady-state tritium permeation (g/day)	Steady-state tritium inventory (kg)
180/100	3×10^8	0.2	4.0
220/100	2.5×10^8	0.16	3.4
180/140	1×10^8	0.8	3.6
380/300	$<10^6$	13.8	0.4
500/500	$\ll 10^6$	95.0	0.09

[a] Breakthrough is defined to occur when 10% of the steady-state rate is reached.

reduced to <0.002 g per day. Note that for a 'clean' inner surface the condition of the outer surface is relatively unimportant for $\alpha_o/\alpha_i \gtrsim 10^{-4}$. This case assumes no damage trapping.

Case 1 is an example of another possible INTOR design with only a bare stainless-steel wall and limiter or divertor. A uniform neutron damage trap concentration (C_t) of one-atomic per cent traps with a detrapping energy (E_t) of 0.85 eV is assumed. The results of the calculations are shown in Fig. VIII-3. The tritium inventory is observed to rise rapidly within the first few years as the neutron damage is decorated by the diffusing tritium. The inventory reaches 2.8 kg within three years, with an eventual steady-state value of 4 kg. No significant permeation is observed for about 10 years of full operation, while the traps are being filled. Once breakthrough is achieved, the permeation rises to a steady-state value of 0.2 g per day.

The baseline steady-state rate of 0.2 g per day is significantly smaller than the 16 g per day calculated by Wienhold et al. [7], primarily because the present operating temperatures are significantly lower than those assumed by Wienhold. The effects of temperature on permeation and inventory are illustrated in Table VIII-2. If the coolant-side temperature is raised, permeation increases. Conversely, if only the plasma-side temperature is raised, the mobile tritium concentration in the implant region is lowered, leading to a lower concentration gradient and hence a lower permeation rate. Clearly, the relatively low permeation rate and high tritium inventory for the INTOR baseline example is primarily due to the low (100°C) coolant temperature. At the more elevated temperatures of commercial power reactors, the calculations indicate that, while the inventory decreases, the tritium permeation problem may reach unacceptable levels if left unchecked.

The first-wall thickness (x_o) and the duty cycle can also affect tritium permeation (Φ_t) and inventory (I_t). In the case of a constant temperature gradient of $143°C \cdot cm^{-1}$ within the wall, the following results have been obtained ranging the wall thickness from 0.35 to 1.4 cm with a fixed temperature $(T_w)_{x_o}$ = 100°C on the outside [3]. The results shown in Table VIII-3 indicate that the values for permeation and inventory at steady state decrease with increasing wall thickness. An increase of the duty cycle as planned in stages 2 and 3 for INTOR has only little influence: tritium permeation and inventory increase by less than 10%.

The tritium permeation and inventory are critically dependent on the assumed values for the molecular recombination rate constant (k_r). The nominal case of Fig. VIII-3 uses a recombination rate constant derived from Eq. (1) with $\alpha = 5 \times 10^{-3}$. Figure VIII-4 shows the calculated permeation and inventory for values of α from 0.5 to 5×10^{-5}. For α = 0.5, more of the incident DT flux recombines into molecules, and less tritium is available to diffuse into the bulk. Hence, the inventory is reduced, and the time to permeation breakthrough is increased. Conversely, for $\alpha = 5 \times 10^{-5}$, there is an increased inventory and more

TABLE VIII-3. INFLUENCE OF WALL THICKNESS AND DUTY CYCLE ON STATIONARY TRITIUM PERMEATION AND INVENTORY WHEN A CONSTANT TEMPERATURE GRADIENT IS APPLIED; t_{stat} IS THE TIME FOR REACHING 90% OF THE STEADY-STATE VALUES

Duty cycle [s/s]		100/146[a]			200/246[a]	
$(T_w)_0/(T_w)_{x_0}$ [°C/°C]	150/100	200/100	300/100	150/100	200/100	300/100
x_0 [cm]	0.35	0.7	1.4	0.35	0.7	1.4
I_t [g]	330	240	100	340	270	110
Φ_t [g·d^{-1}]	0.31	0.088	0.015	0.35	0.097	0.016
t_{stat} [d]	380	610	720	380	610	720

[a] The flux density of 3.3×10^{16} cm^{-2}·s^{-1} has been represented here by:
1.81×10^{16} cm^{-2}·s^{-1} at the duty cycle 100/146, and by
2.20×10^{16} cm^{-2}·s^{-1} at the duty cycle 200/246.

rapid permeation breakthrough. It should be noted that values of the recombination rate constant equivalent to $5 \times 10^{-5} \leqslant \alpha \leqslant 0.5$ have been observed for stainless steel [8].

In summary, for the all-stainless-steel INTOR design the tritium permeation rate after ten years of continuous operation varies from trivial levels ($<10^{-6}$ g per day) to as much as 2 g per day, depending on the materials parameters assumed. Similarly, tritium inventories at the end of life for INTOR are estimated to range from 0.7 to 7 kg, using the same assumption. For the baseline case with a 1.34 cm thick relatively clean stainless-steel wall and no trapping, the inventory is expected to be 1 kg.

Another option for the INTOR design (Case 2) uses a pumped limiter or divertor to intercept all the ion flux and the majority of the tritium charge-exchange neutral flux. Charge exchange to the wall is expected to occur only at a narrow poloidal strip on each side of the limiter or divertor duct. In case both the limiter/divertor plate and the poloidal charge-exchange strips are fabricated from beryllium attached to water-cooled copper substrates, no significant tritium permeation or inventory is expected for the remaining stainless-steel first wall. Hence, tritium permeation and inventory for Case 2 need only to be calculated for the Be/Cu composite. Unfortunately, far less is known about the characteristics of hydrogen

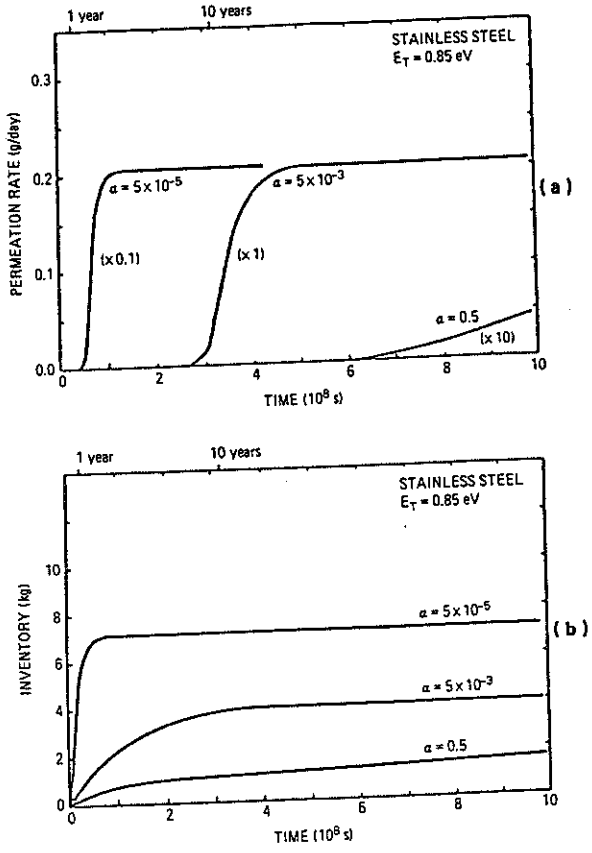

FIG. VIII-4. Effects of molecular sticking coefficient, α, on: (a) permeation rate; (b) inventory. Note the multiplicative factors for the various permeation rate curves.

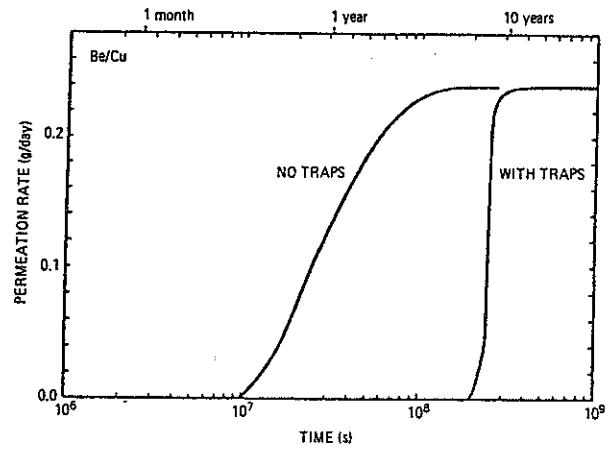

FIG. VIII-5. Permeation rate as a function of time for Be/Cu limiter or divertor plate (INTOR Case 2) with and without the assumed neutron damage traps.

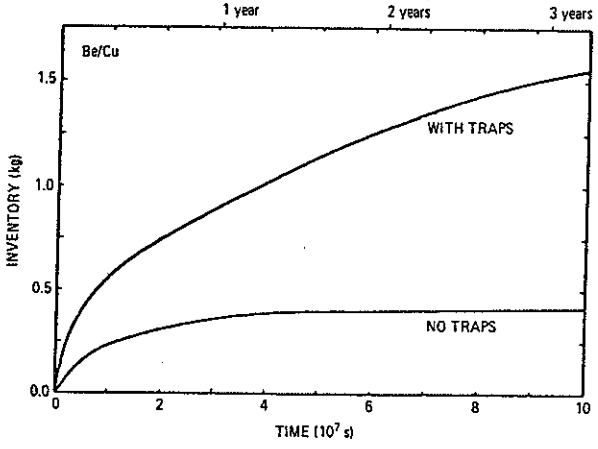

FIG. VIII-6. Inventory as a function of time for Be/Cu limiter or divertor plate (INTOR Case 2) with and without the assumed neutron damage traps.

in beryllium than in stainless steels. Table VIII-1 lists the parameters used in the limiter/divertor calculations. The diffusivity and solubility are from the work of Jones [13]. Since no data are available for the recombination rate constant for beryllium, Eq. (1) is used with $\alpha = 0.5$. The neutron damage trap energy is based on recent ion damage measurements by Wampler. The trap concentration of one-atomic per cent is arbitrary. In fact, ion implantation produces a saturation concentration of as much as 0.4 D/Be over the ion range and may represent a second-phase hydride-like precipitate. Hence, the trapping in beryllium could be much higher than in the present calculations. The beryllium is assumed to be 100% dense and crack-free, and the interface between the Be and Cu is continuous. The lifetime before the component change-out is estimated to be $\lesssim$ three years.

Figure VIII-5 shows the calculated permeation rate. Without neutron damage, breakthrough occurs within half a year and reaches a value of 0.23 g per day by the end of the lifetime. However, when the hypothetical neutron traps are included, breakthrough does not occur for ten years.

The tritium inventory calculations are presented in Fig. VIII-6. With neutron trapping, the inventory reaches 1.5 kg within three years. Even without traps, however, the inventory equals 0.4 kg solely due to the mobile tritium atoms in the bulk. The mobile concentration is as much as $\cong 0.003$ DT/Be because of the enormous DT flux (3×10^{18} DT $cm^{-2} \cdot s^{-1}$) impinging on the limiter/divertor plate. Since the measured solubility of beryllium is only $\cong 6 \times 10^{-6}$ atom fraction/$\sqrt{\text{atm}}$ [13], this implantation-induced concentration is equivalent to a pressure of over 200 atm. Conceivably, this set of conditions could lead to precipitation of a brittle hydride phase or to massive exfoliation from overpressurized voids or non-interconnected porosity. On the other hand, microcracking (crazing) or deliberate connected microporosity (e.g. from plasma spraying) would provide short-circuit pathways for release of implanted tritium. Permeation might be virtually eliminated, and lowered inventories could also be realized. Hence, based on the extremely limited data base for hydrogen in beryllium and the lack of a detailed micro-structural description, it is difficult to calculate any meaningful values for tritium permeation and inventory in INTOR with a Be/Cu composite limiter.

Other materials, notably W/Cu, for the limiter/divertor were investigated although in less detail than Be/Cu [3, 4, 26]. The results indicated that tritium permeation and inventory for other materials were comparable to those for Be/Cu.

2.1.4. First-wall permeation barriers

It is likely that low-Z coatings, e.g. C, TiC, TiB_2, etc. on the inner wall may reduce the tritium permeation rate. A number of implantation studies have shown that such coatings essentially trap all implanted hydrogen atoms until a critical hydrogen lattice concentration is reached. Any additional implanted hydrogen is then released at the implant surface. A second possibility of reducing the

TABLE VIII-4. CALCULATED STEADY-STATE TRITIUM PERMEATION RATES FOR STAINLESS-STEEL WALLS OPERATED WITH A 573K/373K TEMPERATURE GRADIENT. ALL COATINGS ARE 10 μm THICK.

First wall	Tritium permeation ($g \cdot d^{-1}$)
Stainless steel	0.50
SS/Au	1.18×10^{-5}
SS/W	4.0×10^{-8}
SS/Al_2O_3	1.85×10^{-16}
SS/Si	4.15×10^{-20}

permeation is the use of thin metallic coatings (e.g. Pd) on the inner surface to enhance recombination.

The permeation rate can also be lowered significantly by using permeation barriers at the outer surface. Table VIII-4 summarizes the results of calculations for a bare stainless-steel first wall (with a 300 to 100°C temperature gradient, $\alpha_i = \alpha_0 = 5 \times 10^{-5}$), compared to similar first walls with 10 μm thick coatings of Au, W, Al_2O_3 or Si on the outer surface. Literature permeation rates through these coatings were extrapolated to 100°C.

It is also possible that naturally occurring or chemically induced oxides on the stainless-steel water coolant interface can reduce permeation. Figure VIII-7 [3] shows the permeability of deuterium as a function of temperature for HNO_3-passivated 316L stainless steel.

Films formed on HNO_3-passivated austenites are more homogeneous than those due to air exposure, and include more chromium oxide. Thus, at constant temperatures, under the small stresses due to gas pressure, permeation is slightly decreased. On the other hand, this beneficial effect can immediately disappear when the permeation membrane is cycled thermally and by successive removals and applications of D_2 pressure (Fig. VIII-7).

Likewise, for a very thick-oxide-coated 304 SS, permeability is decreased below 350°C. Going above 400°C and back to 210°C no longer shows an oxide influence on permeability (Fig. VIII-8).

When the applied pressure p is twice the pressure π necessary to locally exceed the flow stress at the permeation disc and anchorage, a D_2 permeation is measured at 210°C (Fig. VIII-8), whereas, even after several days, none is detected by mass spectrometry for discs stressed to a lower level.

The tritium permeation rates could be made acceptably low for the INTOR design by the use of these permeation barriers. The viability of coatings or oxides

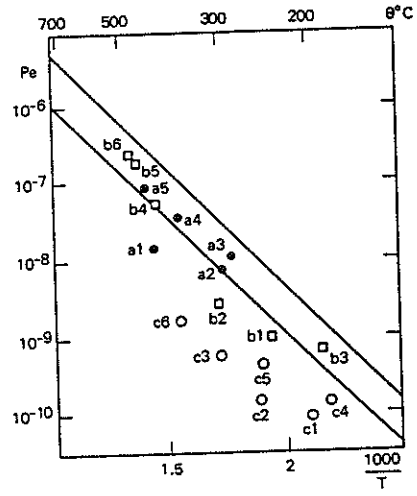

FIG. VIII-7. HNO_3-passivated 316L specimens ●a □ b ○ c. Deuterium permeability: ($cm^3 \cdot cm^{-2} \cdot cm \cdot s^{-1} \cdot bar^{-1/2}$); a1, a2, b3 . . . indicate successive measurements at different temperatures or successive runs at a given temperature θ.

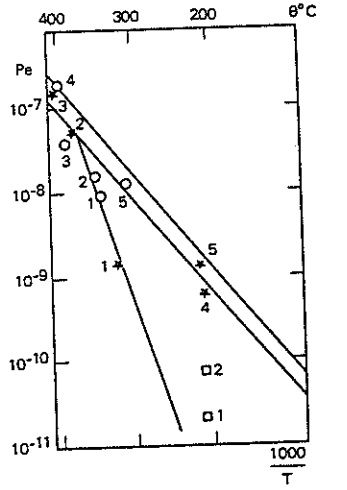

FIG. VIII-8. Thick-oxide-coated 304L. ○ $p < \pi$; □ $p = 2\pi$.

on the outer as well as the inner surface with respect to thermal cycling, coolant compatibility and plasma erosion/re-deposition, etc. remains to be fully investigated. In this respect, permeation experiments employing a Si coating on SS show only one-order-of-magnitude reduction in the permeability, presumably due to the presence of defects in the silicon [14].

2.1.5. Gas release during dwell time and maintenance

As was shown in Section 2.1.3, tritium is expected to permeate into the first wall and limiter or divertor during INTOR operation. This dissolved tritium could be the source of outgassing in the reactor between burns or release to the reactor building during torus repair and maintenance. It is, therefore, necessary to evaluate the magnitude of such a release and what effect, if any, bakeout of the torus components might have in minimizing such a release.

An estimate of the amount of tritium released into the plasma vacuum vessel without bakeout during reactor maintenance was made [4]. The total amount of released tritium depended on the time required for maintenance and was 270 Ci, 390 Ci, and 660 Ci for 4, 8, and 24 hours, respectively, for a stainless-steel vessel at 50°C.

Calculations were also made to determine the effectiveness of torus bakeout. It was shown that a 24-hour bakeout of a stainless-steel first wall at 150°C could reduce the tritium solubility in the first 10^{-3} cm by an order of magnitude. Tungsten, on the other hand, required a 48-hour bakeout at 500°C to reduce the tritium solubility by a factor of 60 at a depth of 3×10^{-2} cm.

Calculations were also performed with the TRIT code to determine the outgassing rate into the vacuum chamber from a stainless-steel first wall for various operating and shut-down conditions [3]. These results are shown in Table VIII-5.

The calculations show that, at end-of-life conditions (i.e. stage 3 = 34 100 h of operation), the quantity of tritium retained in the first wall is 77 $Ci \cdot m^{-3}$. After 100 h of outgassing at 350°C the residual tritium in the first wall is 47 $Ci \cdot m^{-3}$ and 25 $Ci \cdot m^{-3}$ has been released to the torus vacuum chamber.

Unfortunately, the TRIT code does not include the recombination process of hydrogen on the surface, which plays – after shut-down of the discharge – the most important role when the time increases. Therefore, the results given here are to be understood as very preliminary until the calculations with other codes (PERI, DIFFUSE) have been done.

As a result of these calculations it can be seen that outgassing from the first wall could be a major source of tritium in the reactor building during torus maintenance. Calculations have also shown that bakeout of the torus components at elevated temperature can be used effectively to reduce this release.

TABLE VIII-5. OUTGASSING RATES FROM THE FIRST WALL, $Ci \cdot m^{-2}$ (TRIT) Stainless steel, exposure at 300°C, outgassing at 350°C; Stage 1B (2700 h), Stage 2 (8200 h), Stage 3 (34 100 h); FNO = the quantity retained ($Ci \cdot m^{-2}$); FJO = the quantity released toward the blanket side ($Ci \cdot m^{-2}$); t = first-wall thickness.

Time of outgassing (h)			0	1	10	100	1000
1B	t = 3 mm	FNO	15	12	7.1	5.5×10^{-2}	0.0
		FJO	0	0.15	1.6	5.0	5.0
	t = 13 mm	FNO	54	52	47	32	2.4
		FJO	0	1.2×10^{-2}	2.2×10^{-1}	2.6	15
2	t = 3 mm	FNO	18	15	8.4	6.5×10^{-2}	0
		FJO	0	1.9×10^{-1}	1.9	5.9	5.9
	t = 13 mm	FNO	77	74	68	47	3.5
		FJO	0	4.5×10^{2}	4.5×10^{-1}	4.5	24
3	t = 3 mm	FNO	Same values as for Stage 2				
		FJO					
	t = 13 mm	FNO	Same values as for Stage 2				
		FJO					

2.1.6. Radiation effects

The effects of ionizing radiation on tritium permeation and retention in fusion reactor structures are not well understood. It is generally agreed that neither upper limits on the permeation-magnifying effects of ionizing radiation nor the effects of bulk and surface changes to materials due to neutron irradiation have been determined. A review of available literature reporting experimental observations of radiation effects on tritium permeation and retention was made [5]. Additionally, there have been few theoretical studies addressing this issue. Combining this information, several inferences, but only few definite conclusions seem to be possible.

The permeation rate enhancements observed have generally been in non-metallic materials such as oxides and carbides, where the activation energy for diffusion is relatively high. In these cases, electromagnetic radiation (photons) appears to stimulate the movement of hydrogen atoms within the crystal lattice, thus generating a pseudo-diffusivity. When permeation rate accelerations in metals have been seen, the effect is believed to be due to activity in the surface oxide layers. Similar phenomena have been postulated for neutron irradiation, but there are no actual observations. A related effect (photodesorption) has been seen on surfaces where single gas atoms were ejected rather than awaiting the recombination to form molecules which is normally required for gas exhalation.

It is difficult to accurately quantify these processes, but it is believed that cross-sections for photodesorption and detrapping are less than 10^{-18} cm^2. If the temperature of the first wall and limiter/divertor is high enough it appears that radiation effects on permeation rate will be inconsequential, compared with thermal processes. For graphite or carbides, there may be an observable effect, but these materials are comparatively impermeable to begin with, so, again, it does not appear that radiation effects will be deleterious to the permeation rate. Indeed, they may actually make it easier for implanted tritium to return to the plasma, thereby reducing losses to coolant streams. It should be emphasized, however, that the experimental data are not sufficient to allow firm conclusions.

A steady-state analytical model was developed which contains parameters associated with the radiation processes of detrapping, photo-desorption, and diffusivity enhancement. Multiple traps and two simultaneously diffusing hydrogen isotopes are also accommodated. Results support the conclusion that electromagnetic radiation will not significantly affect tritium permeation rates in stainless-steel structures.

A more serious problem is tritium retention. A major contributor to the total site inventory will be tritium retained in the first wall and other interior structures, tritium trapped in voids or bubbles and chemically bound to impurities in metals. Neutrons are known to produce a variety of material defects, including vacancy-interstitial pairs, dislocations, voids, and transmutations. There has been some suggestion [5] that structural defects may saturate such that tritium atoms could be trapped at about 1% of the lattice sites in stainless steels based on observations of the effects of high-energy protons and deuterons. Besides the structural damage caused, neutron irradiation will produce hydride formers such as Ti, V, Nb, Zr in 316 stainless steel. These could result in inventories of hundreds of grams per megawatt-year of reactor operation.

Unfortunately, there are few experimental data on neutron effects on such trap formation. Experiments with neutron-irradiated titanium showed sorption rate constants and hydrogen solubilities greater than for unirradiated specimens [13]. Experiments in the USSR [6] suggest that voids formed by neutron irradiation could result in a first-wall tritium inventory of ten or more kilograms. Other

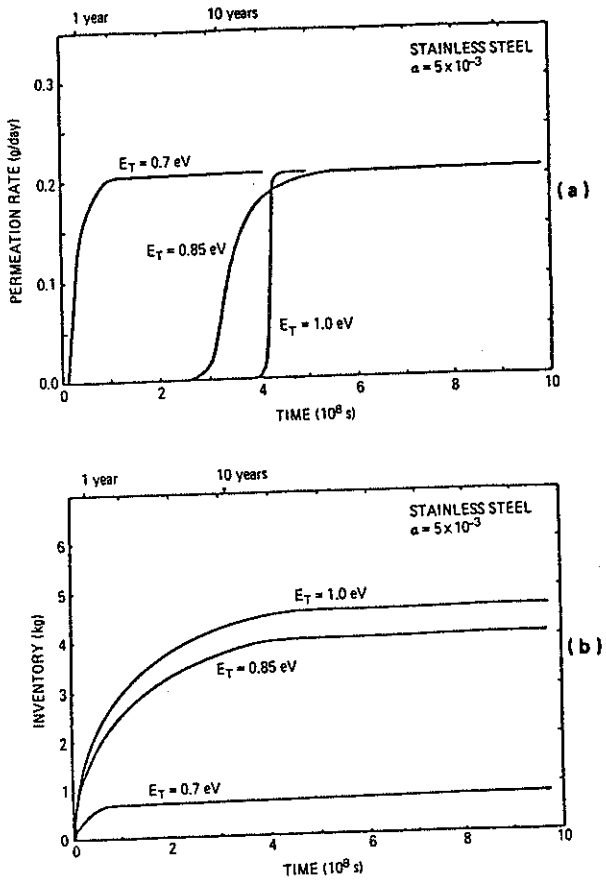

FIG. VIII-9. Effects of the neutron damage detrapping energy on: (a) permeation rate; (b) inventory.

experiments [4] show that X-ray irradiation can enhance the release of hydrogen from a stainless-steel sample after cathodic hydrogen charging.

The assumptions for neutron damage trapping also affect the tritium permeation and inventory calculations. A uniform trap concentration, C_T, of one-atomic per cent traps with a detrapping energy, E_T, of 0.85 eV is assumed in the baseline case. The traps are considered present from zero time rather than

evolving with time. Comparison of the INTOR dpa rate with ion implantation experiments indicates that the bulk neutron trap concentration could approach saturation in times of much less than one year. Detrapping energies of 0.7 to 0.9 eV are observed in deuterium-bombarded stainless steels, while a value of 1.0 eV has been reported for helium ion damage. The effects of detrapping energies from 0.7 to 1.0 eV are shown in Fig. VIII-9. Besides lowering the inventory, the time to permeation breakthrough is significantly reduced for smaller values of E_T. Of course, neutron trapping may be quite different from light-ion damage.

To summarize, it appears that radiation fields will not have a significant effect on tritium permeation rates. If traps are formed at sufficiently high rates, however, the radiation may prevent breakthrough for the life of the component. Radiation may also assist in desorption on the plasma side to further reduce permeation.

For impermeable materials such as metal oxides and carbides, the effective diffusivity may be increased, but it is not clear that this will pose a problem in practice. Inventories of tritium in interior fusion reactor structures are likely to be substantially increased by neutron-induced traps such as voids and transmutation products, but there are insufficient data for confidence in quantitative estimates.

2.1.7. Conclusions

Tritium permeation through the first wall and/or limiter/divertor will be the primary source of tritium in the coolant. Using available models, an attempt was made to predict the tritium permeation rate and the associated tritium inventory for the materials used in the INTOR design. However, surface conditions in a fusion reactor are unknown as are the neutron damage trapping characteristics of most materials. For some materials (Be), even tritium diffusivities and solubilities are uncertain.

For a stainless-steel wall, the tritium permeation rate after ten years of continuous operation ranged from $<10^{-6}$ g per day to 2 g per day. For a Be/Cu limiter or divertor, the permeation rate ranged from $<10^{-6}$ g per day to 0.23 g per day after three years of continuous operation. It is expected that the combined permeation to the coolant will be 0.01 to 1 g per day (100 to 10 000 Ci per day). The tritium inventory in the stainless-steel wall case ranged from 0.4 kg to 7 kg after ten years of continuous operation, and up to 1.5 kg in the limiter/divertor case after three years of continuous operation. For the baseline case with a 1.34 cm thick, relatively clean stainless-steel wall and no trapping, the inventory is expected to be 1 kg.

Tritium permeation rates could be minimized by use of permeation barriers on the inner or outer surfaces but may be unrealistic because of expected physical defects in the coating materials.

Large-torus-component tritium inventories have the potential for release (outgassing) during torus maintenance. Calculations show that this can be minimized by in-situ bakeout of the torus.

2.2. Tritium processing of the primary coolant

As was shown in Section 2.1, 100 to 10 000 Ci per day is expected to permeate through the first wall and limiter/divertor into the primary coolant. This section will review methods of tritium removal from water and compare several methods using capital and operating cost estimates. The allowable tritium concentration in the water coolant was also calculated by using a cost benefit analysis.

2.2.1. Methods for tritium separation from water

There are several technologies available for the separation of tritium from water (tritium from protium). Most of these technologies were originally developed to produce heavy water (deuterium from protium) and have more recently been evaluated for removal of tritium from heavy water (tritium from deuterium). It seems likely that the INTOR first-wall and limiter/divertor coolant systems will be light-water. Use of heavy water would be possible and, in some ways, advantageous.

Many processes were investigated by the INTOR participants for the separation of tritium from the first-wall, limiter and divertor coolant water [3–6]. Of these processes the four that appear most appropriate for this application are: Vapour Phase Catalytic Exchange/Cryogenic Distillation (VPCE/CD), Direct Electrolysis/Cryogenic Distillation (DEL/CD), Combined Electrolysis Catalytic Exchange/Cryogenic Distillation (CECE/CD), and Water Distillation/Electrolysis/Cryogenic Distillation (WD/EL/CD). All four processes use low-temperature (cryogenic) hydrogen distillation for the final isotopic tritium enrichment but differ in the front end process used to transfer the tritium from the water to the elemental form.

Vapour Phase Catalytic Exchange/Cryogenic Distillation (VPCE/CD) uses a countercurrent array of catalytic exchange reactors to transfer the tritium from the water to elemental form, according to the equilibrium reaction:

$$HTO + H_2 \rightleftharpoons H_2O + HT$$

or $$DTO + D_2 \rightleftharpoons D_2O + DT$$

(H = protium, D = deuterium, T = tritium)

Once the tritium has been transferred to the elemental forms (HT or DT), cryogenic distillation is used to make the isotopic separation.

Direct Electrolysis/Cryogenic Distillation (DEL/CD) uses commercially available electrolysis cells to electrolyse all the process feed water to hydrogen and oxygen. The hydrogen with a small amount of tritium is then fed to a cryogenic distillation system where the isotopic separation is performed. The detritiated hydrogen is then recombined with the oxygen, from the electrolysis cell, to form water which is recycled back to the coolant loop.

Combined Electrolysis Catalytic Exchange/Cryogenic Distillation (CECE/CD) differs from the other processes in that the front end (CECE) can perform a significant part of the isotopic separation as well as provide elemental hydrogen feed to the cryogenic distillation back end. This process uses a special Canadian hydrophobic catalyst in a liquid-water gaseous hydrogen counter-flow column.

The final process considered appropriate for this study is Water Distillation/Electrolysis/Cryogenic Distillation (WD/EL/CD). This process uses water distillation to strip tritium from the coolant water and provide slightly enriched water feed to an electrolyser. The hydrogen product from the electrolyser is fed to a low-temperature (cryogenic) hydrogen distillation system for final isotopic tritium enrichment.

All four processes remove tritium from the first-wall, limiter and divertor coolant and are capable of returning the recovered tritium to the primary fuel cycle.

2.2.2. Cost and process comparison

One of the best ways of comparing the various technology options is to compare the capital and operating costs associated with each option. For the four options being evaluated for detritiation of the first-wall coolant, the most important feature to be considered is the process flowrate. The capital cost is strongly dependent on the process flowrate because the flowrate determines the size and, therefore, the cost of the equipment. It is generally believed that the capital cost for this type of system varies to about the 0.6 power with the flowrate. The operating cost is even more dependent on the flowrate.

The process flowrate necessary to detritiate the first-wall coolant depends on the tritium permeation rate and the allowable coolant concentration. In fact, the volume processed is equal to the permeation rate divided by the coolant tritium concentration and the system detritiation efficiency:

$$\text{Volume processed (litres per day)} = \frac{\text{Permeation rate (Ci/day)}}{\text{Coolant conc. (Ci/litre)} \times \text{efficiency (0.0–1.0)}}$$

If the detritiation efficiency is assumed to be one, then the process flowrate can easily be calculated for the permeation rates and coolant concentration of interest.

TABLE VIII-6. CAPITAL AND OPERATING COSTS FOR FOUR OPTIONS

Technology	CECE/CD	DEL/CD	VPCE/CD	WD/EL/CD
Total capital cost ($M)	15	20	25	15
Capital cost 10 years ($M per year)	1.5	2.0	2.5	1.5
Total operating cost ($M per year)	0.75	1.1	2.0	0.83
Total cost ($M per year)	2.25	3.1	4.5	2.33

(all costs in mid-1982 US dollars)

TABLE VIII-7. CAPITAL COST OF CECE/CD OPTION

$L \cdot d^{-1}$	25	100	1000	10 000
Total capital cost of CECE/CD ($M)	2.5	4	15	50

Between 100 and 10 000 $L \cdot d^{-1}$, the capital cost of CECE/CD is:

$$\text{Capital cost CECE/CD in \$M (1982)} \cong 15 \left[\frac{\text{Permeation rate } (Ci \cdot d^{-1})}{\text{Coolant concentration } (Ci \cdot L^{-1}) \times 1000\ (L \cdot d^{-1})} \right]^{0.55}$$

As was mentioned in the introduction, the first-wall permeation rate is between 10^2 and 10^4 Ci per day with a most likely value of 10^3 Ci per day. The recommended coolant tritium concentration is between 0.1 and 10 $Ci \cdot L^{-1}$ with 0.1 $Ci \cdot L^{-1}$ being the most likely. This leads to a process flowrate range of 10^2 to 10^5 L per day with a most likely value of 10^4 L per day.

A rough economic analysis was performed on the four processes previously discussed: CECE/CD, DEL/CD, VPCE/CD, and WD/EL/CD. For the basis of the comparison it was assumed that the permeation rate will be 1000 Ci per day and

the coolant concentration will be 1 $Ci \cdot L^{-1}$. For CECE/CD, DEL/CD, and WD/EL/CD, which have a detritiation efficiency close to one, a process flowrate of 1000 L per day was chosen. For VPCE/CD, which uses a detritiation efficiency of approximately 0.9, 1100 L per day was used. The capital and operating costs for the four options are shown in Table VIII-6.

The capital cost of the CECE/CD option was also estimated for a range of process flowrates. This information is in Table VIII-7; all costs are again mid-1982 US dollars.

It can be seen from Table VIII-6 that the capital and operating costs for CECE/CD and WD/EL/CD are nearly identical. The cost for DEL/CD is slightly higher but certainly competitive. The cost of VPCE/CD is higher by a factor of two than either CECE/CD or WD/EL/CD.

The CECE/CD technology has the advantage of detritiating the water to a concentration that is acceptable for unrestricted release to the environment. This feature becomes important when decommissioning the coolant loop and its 10^5 litres of water. A large CECE/CD system would also be capable of detritiating water from other INTOR sources such as the building detritiation systems and the primary fuel cycle purification system because the CECE/CD has the capability of accepting feeds at different tritium concentrations. The CECE/CD technology does, however, have disadvantages. Of the four options it has the least operating experience, especially at large flowrates. Also, to gain the advantage of lower cost, it does much of the separation in the front end CECE section, which would have to handle tritiated water at a much higher concentration than the other technologies. It should be noted that other parts of INTOR will produce tritiated water, some of which will be of very high concentration.

The WD/EL/CD technology has the advantage of many years of commercial experience, especially for heavy-water production. The distillation process is well understood, and equipment is readily available for the flowrates in question. This option as designed and costed will not provide water suitable for unrestricted release without multiple processing. The WD/EL/CD does allow multiple feed concentrations.

The DEL/CD technology is also a viable option. There is much practical experience with both electrolysis of tritiated water and cryodistillation of hydrogen isotopes although they have not yet been used together on this scale.

The VPCE/CD does not appear to be suitable for tritium recovery from low-level (light) water. All experience with this technology has been with heavy water, and VPCE/CD was the choice of Grenoble and Pickering for heavy-water detritiation. If INTOR or another fusion machine opted for a heavy-water-based coolant system, this technology would be very competitive.

2.2.3. Tritium concentration in water coolant

Tritium permeating into coolant water and subsequent loss of water from the cooling system constitute a potential safety concern for fusion reactors of the INTOR class. Regulations specify the maximum allowable dose to operating staff and to the off-site population. Control systems to reduce tritium concentrations in the primary coolant water and the reactor building air will be needed to ensure that exposures meet these regulations. The requirement for occupational exposure states that doses must be less than 3 rem per quarter and 5 rem per year. To meet this requirement, protective suits will be required for work in concentrations above the maximum permissible concentration of tritiated water in air, 5×10^{-6} $Ci \cdot m^{-3}$. Public exposure is limited to 500 mrem per year at the site boundary. The release limit of 10^4 Ci per year selected for INTOR will produce doses well below this regulation if a suitable exclusion area is used. In addition to these specific requirements, exposures are required to be as low as reasonably achievable (ALARA).

The most logical means of determining the maximum allowable tritium concentration in the coolant would be an optimized economic analysis that considers all appropriate factors. The costs that should be considered include: the cost of the reactor hall atmosphere detritiation system, the cost of the water coolant detritiation system, the cost of reducing, collecting and returning water leakage, and the cost of decreased labour productivity when protective suits are necessary for operations. At this stage of INTOR, there is insufficient design detail to accurately define all relevant costs. In the absence of desired detail, a less sophisticated analysis is used.

It was estimated, in Section 2.1, that the rate of tritium permeation into the coolant would be 100 to 10 000 Ci per day with a most likely value of 1000 Ci per day. It was also shown, in Section 2.2, that coolant water detritiation systems as large as 10 000 L per day are technically feasible and economically acceptable. If the average permeation rate is 1000 Ci per day and the detritiation system can process 10 000 L per day, the resultant concentration of tritium in the coolant water will be 0.1 $Ci \cdot L^{-1}$. Based on heavy-water reactor experience and taking into consideration the special INTOR design features for frequent assembly and disassembly of the torus, the unrecoverable water leakage for INTOR is estimated to be 10 L per day. If the tritium concentration in the coolant is maintained at 0.1 $Ci \cdot L^{-1}$ the resulting loss to the reactor hall will be about 1 Ci per day. This quantity, if released directly to the stack, would be well within the accepted INTOR design release of 10–20 Ci per day. If the reactor room is 1.8×10^5 m^3 and is ventilated at two volume changes per day the average gaseous tritium concentration in the reactor hall would be only 3 $\mu Ci \cdot m^{-3}$. This concentration would allow access, if limited only by tritium dose rate, to the reactor hall without air-supplied protective suits.

The INTOR coolant system has an estimated total volume of 60 to 200 m^3. At 0.1 $Ci \cdot L^{-1}$, this volume will contain 0.6–2.0 g of tritium which if completely lost would be within the maximum acceptable release to the reactor hall.

It might be necessary to allow the coolant concentration to reach a level above 0.1 $Ci \cdot L^{-1}$ if the permeation rate exceeds 1000 Ci per day. This occurs because the maximum practical size for the coolant detritiation system is 10 000 L per day. This should be avoided, if at all possible, because of the resulting deleterious effect on the reactor hall detritiation system and the access to the reactor hall. If, as an example, the coolant concentration was 1.0 $Ci \cdot L^{-1}$ the tritium inventory in the coolant could be 20 g and the unprocessed release to the stack could be 10 Ci per day.

For these reasons the INTOR water coolant concentration should have a design value of 0.1 $Ci \cdot L^{-1}$. This, however, should be reviewed if further studies show that the permeation rate exceeds 1000 Ci per day, or if sufficient detailed design information exists to permit an optimized economic analysis.

2.3. Conclusions and recommendations

Investigation of tritium permeation and inventory in the first wall, limiter and divertor indicates large uncertainties in a number of areas. For all plasma-side materials, characterization of the surface conditions in the actual reactor environment and the effects of neutron damage trapping result in a large uncertainty in both tritium permeation and inventory. For some materials, tritium diffusivities and solubilities are highly uncertain.

The best estimate that can be provided at present for the steady-state tritium permeation rate to the coolants of first wall, limiter and divertor is in the range of 10^2 to 10^4 Ci per day. The recommended tritium concentration in the coolant water is 0.1 $Ci \cdot L^{-1}$.

Several methods for separating tritium from water are available. The capital and operating costs are strongly dependent on the process flow rate which is proportional to the permeation rate and varies inversely with the allowable tritium concentration in the coolant loop. For a permeation rate of 10^3 Ci per day and a coolant concentration of 0.1 $Ci \cdot L^{-1}$, the volume of coolant water processed would be 10 000 L per day. The corresponding capital cost is approximately \$50 M with an operating cost of approximately \$2 M per year.

It is concluded that tritium permeation is not a feasibility issue but remains critical to the INTOR design. However, the economic penalty can be seriously large if the tritium permeation rate is larger than 10^4 Ci per day. Serious R and D is required to develop an adequate data base for tritium permeation. A clear goal for the first-wall/limiter/divertor designs and for R and D programmes is to ensure that the tritium permeation rate is less than 10^4 Ci per day. The time to reach steady-state levels for the tritium inventory and permeation rates can be long,

depending on neutron damage trapping, ranging from less than a year for no trapping to greater than ten years for severe trapping. This can be an important consideration for components with short life such as the limiter and divertor. The estimated end-of-life tritium inventory in the first wall, limiter and divertor is in the range of 0.1 to 1.0 kg. Future effort should address the concerns associated with a significant build-up of tritium inventory in the in-vessel components.

3. TRITIUM CONTAMINATION OF REACTOR ENVIRONMENT

Tritium leakages into the reactor room will occur during normal operations, maintenance operations and accidents. The personnel access for maintenance is desired 24 hours after the reactor shutdown. Personnel protection of some level is required in relation to the tritium concentration level in the reactor room. However, the degree of protection affects worker productivity, and the tritium concentration level to be maintained also significantly affects the capital and operating costs associated with the air detritiation system.

In the following, the problems of tritium contamination of the reactor environment are discussed [3–6].

3.1. Sources of tritium contamination

The main tritium sources in the reactor room for normal, maintenance and accident conditions are identified as follows:

- Normal
  - Leakages from coolant lines
  - Leakages and permeation from the plasma chamber and associated components
  - Leakages from tritium systems
- Maintenance
  - Same as normal
  - Outgassing from equipment in the reactor room
  - Leakages from disconnections
- Accident
  - Fuellers
  - Pumps
  - Blanket recovery lines
  - Primary coolant
  - Others

TABLE VIII-8. ESTIMATED RANGES OF TRITIUM RELEASES IN THE REACTOR ROOM[a]

Systems/conditions	Normal ($Ci \cdot d^{-1}$)	Maintenance ($Ci \cdot d^{-1}$)	Accident (Ci)
Torus	$10^{-2} - 20$	–	$<10^3$
Limiter/divertor	–	$<10^3$	–
First wall/blanket	–	$<10^3$	$<10^5$
Diagnostics	$10^{-2} - 10^{-1}$	<50	$<10^3$
Fuellers	$10^{-2} - 5$	$10 - 10^2$	$<2 \times 10^5$
Blanket recovery lines	$10^{-2} - 10^{-1}$	<10	$<2 \times 10^4$
Pumps	$10^{-2} - 10^{-1}$	<50	$10^{-2} - 10^5$
Primary coolant (H_2O)			
Lim/Div/FW	<6	2 – 210	$<10^5$
Shield	<0.2	≈1	30 – 60
Blanket	<0.2	≈1	$<10^5$
Total	<30	$<10^3$	$<10^5$

[a] Based on data of Ref. [5] and corrected.

The estimated possible ranges of tritium sources in the reactor room for normal, maintenance and accident conditions are summarized as follows:

- Normal <30 Ci per day
- Maintenance $<10^3$ Ci per day
- Accident $<10^5$ Ci

The dominant leakage during normal operation comes from the primary coolant of the first wall and limiter/divertor, fuellers, and torus sector. An alternative to be considered in future INTOR design would be to limit the total tritium leakage in the reactor room to less than 10 Ci per day. During maintenance, large releases of tritium could occur from several systems ($50 - 10^3$ Ci). Among these systems, limiter/divertor and first wall/blanket can be the most important, as high as 10^3 Ci per day. A breakdown of estimated releases of tritium source terms [5] is shown in Table VIII-8.

The following design approaches should be taken to minimize tritium leakage:

- Design of coolant lines to minimize leaks
- Application of multiple containment system
- Minimum tritium inventory in all components
- Design of welds, seals and components to minimize leaks
- Design to minimize tritium permeation

3.2. Tritium concentration levels in air

The tritium concentration level in the reactor room is desired to be maintained down to the level to permit personnel access 24 h after reactor shutdown under normal, maintenance and accident conditions.

Under normal conditions, it is desirable that the tritium concentration in the reactor room be maintained low enough to allow access without protective suits. For this purpose, there are two possible methods of purifying the reactor room air: (i) changing continuously and rapidly the room atmosphere with a high-speed ventilation and releasing the contaminated air through a stack, (ii) processing and recycling the room air through an air detritiation system. In the former method, the impact on the environment should be considered carefully, and in the latter one, the cost of the detritiation system may be excessive from an economical viewpoint because the capacity of the system becomes large when a low tritium concentration level associated with a high leak rate is required.

The tritium leakage rate estimated in Section 3.1 makes it unacceptable to release the tritium into the environment through the ventilation system, even under normal conditions; if, however, the tritium release could be limited to below 10 Ci per day, the reactor room could be ventilated directly to the stack without exceeding the INTOR design limit of 10 000 Ci per year. Here, the flow rate of the air detritiation system required for normal conditions was estimated [4, 5]. Figure VIII-10 shows the effects of the tritium leakage rate into the reactor room under normal conditions and the tritium concentration level in the reactor room on the flow rate of air detritiation system. It is clear from the figure that a detritiation system of 2.5×10^5 m^3 per hour is required to maintain the tritium concentration level in the reactor room at 5 $\mu Ci \cdot m^{-3}$ when a tritium leakage rate of 30 Ci per day is assumed.

Under maintenance and accident conditions, protective suits may be required for personnel access 24 h after reactor shutdown if the tritium leakage rates estimated in Section 3.1 are taken into account. To examine the flow rate of the air detritiation system required for personnel access 24 h after reactor shutdown under accident conditions, sensitivity of the flow rate to the following variables was studied: clean-up time, amount of tritium released, rate of formation of HTO

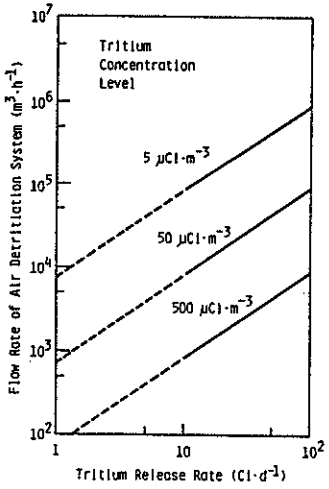

FIG. VIII-10. Required flow rate of air detritiation system under normal conditions as a function of tritium release rate and concentration level (air detritiation system may not be needed in the case of tritium release rate of ≤10 Ci·d⁻¹).

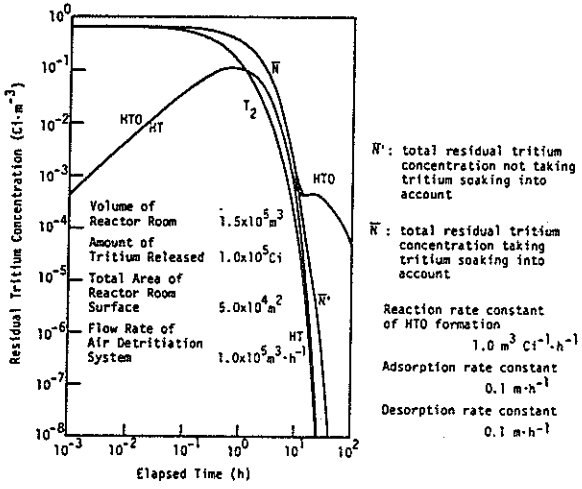

FIG. VIII-11. Tritium clean-up characteristics.

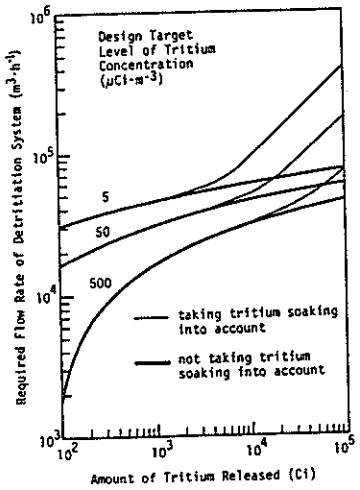

FIG. VIII-12. Required flow rate of air detritiation system in the event of tritium release.

from HT or T_2, rate of adsorption/desorption at the wall surface of the reactor room, volume of the reactor room, design target level of tritium concentration.

Figure VIII-11 shows the tritium clean-up characteristics. As is seen in this figure, the residual tritium concentration level in the reactor room is not reduced as would be expected according to tritium soaking. The effect of the design tritium concentration level after 24 h of shutdown in the reactor room on the required flow rate of the air detritiation system is shown in Fig. VIII-12.

In the event of an accidental tritium spill of 10^5 Ci, air detritiation systems of 4.5×10^4 m³ per hour and 8.1×10^4 m³ per hour are to be provided to clean up reactor rooms of 1.5×10^5 m³ and 3.0×10^5 m³, respectively, below an activity level of 500 μCi·m^{-3} in 24 h, not taking account of tritium soaking. When, however, the tritium soaking into the reactor room walls is taken into account, the flow rate of the detritiation system could increase remarkably. It is preferable to design the reactor rooms providing minimum HTO formation, minimum surface adsorption and a reasonable desorption.

3.3. Air detritiation system and cost

An air detritiation system consists of the following main pieces of equipment: blower, air pre-heater, catalytic reactor, aftercooler, and water removal system. A schematic of the process [4] is shown in Fig. VIII-13.

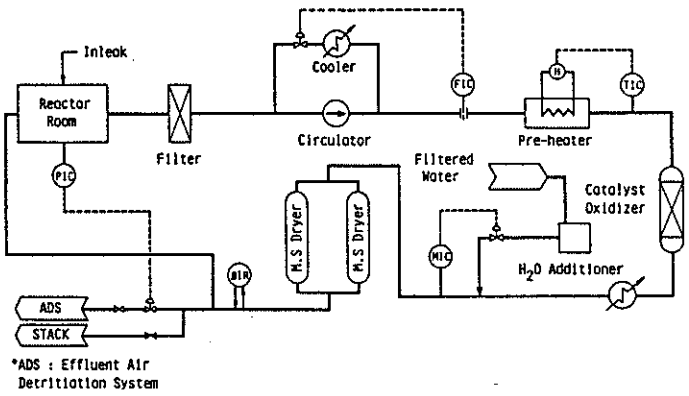

FIG. VIII-13. Flow sheet of air detritiation system.

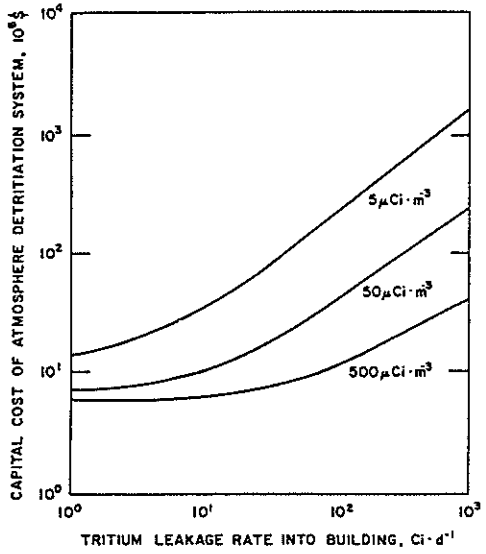

FIG. VIII-14. Tritium concentration levels in the reactor room atmosphere as a function of leak rate and capital cost.

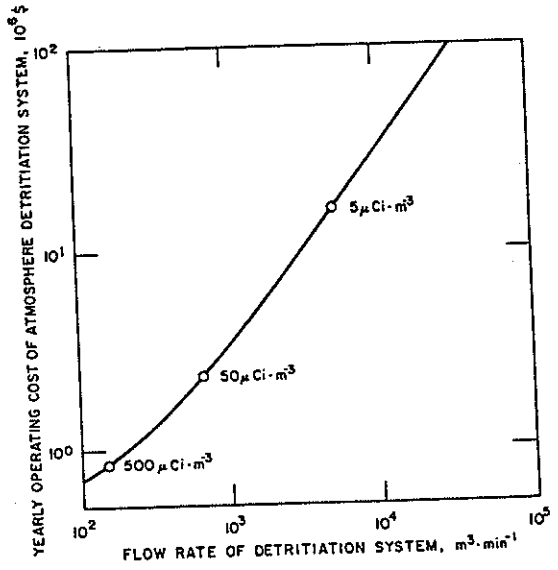

FIG. VIII-15. Tritium concentration levels in the reactor room atmosphere as a function of flow rate and yearly operating cost at a tritium leakage rate of 30 Ci·d^{-1}.

The cost of the air detritiation system is evaluated here [26]. The total cost of the detritiation system is divided into two categories: total capital cost and annual operating expenses. The total capital cost is the sum of the detritiation system cost, the cost of the building containing the system, and the cost of a tritiated-water recovery unit. The capital cost to maintain a given concentration is shown as a function of the leak rate in Fig. VIII-14. As is evident from Fig. VIII-14, the total capital cost rises quickly with increasing leak rate. At 30 Ci per day, about 15 million dollars are required to maintain 50 μCi·m^{-3}. The cost increases by a factor of five to maintain 5 μCi·m^{-3}, whereas it decreases by a factor of two to maintain 500 μCi·m^{-3}. The annual operating cost as a function of the total system flow rate is shown in Fig. VIII-15. The annual operating cost consists of utilities and manpower.

As is shown in Fig. VIII-15, the annual operating cost of the appropriate system ranges from about 14 million dollars a year to maintain 5 μCi·m^{-3} down to about 0.45 million dollars for 500 μCi·m^{-3}. Thus, in ten years, the combined

capital and operating costs to maintain 5, 50 and 500 $\mu Ci \cdot m^{-3}$ (or to reach these levels at any time) are 210, 32 and 11 million dollars with associated worker efficiencies of 1, 0.5 and 0.5, respectively.

3.4. Personnel access

Determination of the tritium concentration level in the reactor room is a delicate problem because personnel access, environmental safety and cost of the air detritiation system should be considered.

It is desirable that the air detritiation system maintain the tritium concentration levels in the reactor room in the following ranges, for given tritium leak rates under normal, maintenance and accident conditions, 24 h after reactor shutdown:

- Normal $<5\ \mu Ci \cdot m^{-3}$ (in HTO form)
- Maintenance and accident $<500\ \mu Ci \cdot m^{-3}$

In normal conditions, when personnel access 24 h after reactor shutdown without protective suits is desirable, the tritium concentration level must be maintained below 5 $\mu Ci \cdot m^{-3}$. Access without protective suits 24 h after reactor shutdown may not be economically reasonable if the cost of the detritiation system required to maintain the tritium concentration level below 5 $\mu Ci \cdot m^{-3}$ for a tritium leakage rate of 30 Ci per day is taken into account.

There are three possible strategies for personnel access in normal conditions, and the selection of the strategy depends on the tritium leakage rate in normal conditions. Further investigation is required in this area. Three strategies are:

(1) Personnel access without protective suits is intended by maintaining the tritium concentration level in the reactor room below 5 $\mu Ci \cdot m^{-3}$ by using a ventilation system. For this purpose, the tritium leakage rate into the reactor room should be reduced to a level of less than 10 Ci per day for which direct release to the environment through a stack is permitted.
(2) Personnel access without protective suits is intended by maintaining the tritium concentration in the reactor room below 5 $\mu Ci \cdot m^{-3}$, using an air detritiation system. For this purpose, the tritium leakage rate into the reactor room should be reduced to a level of about 15 Ci per day for which an economically reasonable detritiation system ($\approx$40M \$) can be designed.
(3) Personnel access with protective suits is intended at tritium concentration levels of above 5 $\mu Ci \cdot m^{-3}$ up to 500 $\mu Ci \cdot m^{-3}$. In this case, an economically reasonable detritiation system can be adopted for a tritium leakage rate of 30 Ci per day.

For tritium leakage in maintenance and accident conditions, the tritium concentration in the reactor room 24 h after reactor shutdown is larger than

TABLE VIII-9. WORKING ENVIRONMENT AND PROTECTIVE CLOTHING REQUIREMENTS

Room concentration	Surface contamination	Clothing required	Efficiency
≈ 0 (uncontrolled areas)	≈ 0	None	100%
$<5\ \mu Ci \cdot m^{-3}$	<50 counts$\cdot$min^{-1}	smock and shoecovers	71%
$<5\ \mu Ci \cdot m^{-3}$	50–10000 counts$\cdot$min^{-1}	2 pc. blues and gloves	56%
$5-500\ \mu Ci \cdot m^{-3}$	No water > 1 Ci$\cdot L^{-1}$	Bubble suit and supplied air	50%

1 MPC[1] ($5\ \mu Ci \cdot m^{-3}$) even if the air in the reactor room is processed by a practicable detritiation system. In maintenance and accident conditions, therefore, some protection suits are required for personnel access. In some extreme accident conditions, it may not be possible to enter the reactor room even with protective suits.

The tritium concentration in the reactor room will determine the amount of time and the types of protective clothing required for personnel who work in it. Personnel access can be allowed up to a tritium concentration of 500 $\mu Ci \cdot m^{-3}$ by wearing bubble suits with an independent air supply. Bubble suits provide a safety factor of at least 100 against tritium [5], which means that a worker in a bubble suit can be allowed to work in a 500 $\mu Ci \cdot m^{-3}$ environment for the same length of time as an unprotected worker in a 5 $\mu Ci \cdot m^{-3}$ environment. Therefore, even in the event of accidents, the tritium concentration level is to be maintained below 500 $\mu Ci \cdot m^{-3}$. The efficiency of a worker in a bubble suit decreases by a factor of 2 [4, 5]. The relationship between protective clothing and efficiency is summarized in Table VIII-9. The reduction in the productivity of maintenance personnel due to the use of bubble suits should be included in the availability estimate for the reactor. The use of robotic units during the wait time for activation gamma-ray decay and detritiating the reactor room atmosphere is proposed to improve device availability.

[1] MPC stands for 'maximum permissible concentration'.

4. TRITIUM-BREEDING BLANKET

At present, several types of materials are known which can be used for tritium breeding in the INTOR blanket. These are mostly ceramics: Li_2O, $LiAlO_2$, Li_3SiO_4, L_2ZrO_3, Li_2TiO_3; lithium-lead eutectic ($Li_{17}Pb_{83}$) is considered as well. All these materials have sufficient lithium atom density and acceptable sets of physical, chemical and mechanical properties to be used in the blanket. Critical issues related to the implementation of the materials will be discussed in this section.

4.1. Solid breeder materials

All the ceramics listed above were considered. Their common feature is sample cracking under irradiation. Such cracking may result in extra thermal resistivity and abnormal temperature, which could result in exceeding the upper temperature limit, sintering and reduced tritium recovery.

4.1.1. New data on solid breeder materials properties

a. Physical properties

Recently, new data on Li_2O properties have been obtained from the research programmes at JAERI (Japan) and ANL, GA (USA) [5]. The basic physical properties of Li_2O adopted for the time being are summarized below.

Li_2O properties

Density ($g \cdot cm^{-3}$)	2.01
Lithium density ($g \cdot cm^{-3}$)	0.93
Melting temperature (°C)	1430

b. Thermal conductivity

Formulas for the thermal conductivity $K (W \cdot cm^{-1} \cdot K^{-1})$ calculation depending on the porosity p^a are given in Table VIII-10. According to Fig. VIII-16 the thermal conductivity of Li_2O is twice that of $LiAlO_2$ [25].

c. Heat capacity

The results of heat capacity measurements for ceramics can be extrapolated by formulas given in Table VIII-11. The heat capacity of all ceramics increases with temperature growth. Li_2ZrO_3 has the lowest heat capacity (Fig. VIII-17) [25].

TABLE VIII-10. THERMAL CONDUCTIVITY OF CERAMICS, $K = K_0 + \frac{1 - p^a}{1 + Bp^a}$

Material	K_0, $W \cdot cm^{-1} \cdot K^{-1}$	B
Li_2O	$(1.4 + 0.01828\ T)^{-1}$	$1.95 \times 10^{-4}\ T$
$LiAlO_2$	$0.0147 + 9.43/T$	$1.95 \times 10^{-4}\ T$
Li_4SiO_4	$0.0198 + 8.5/T$	$1.95 \times 10^{-4}\ T$
Li_2ZrO_3	$0.0102 + 6.68/T$	$1.95 \times 10^{-4}\ T$

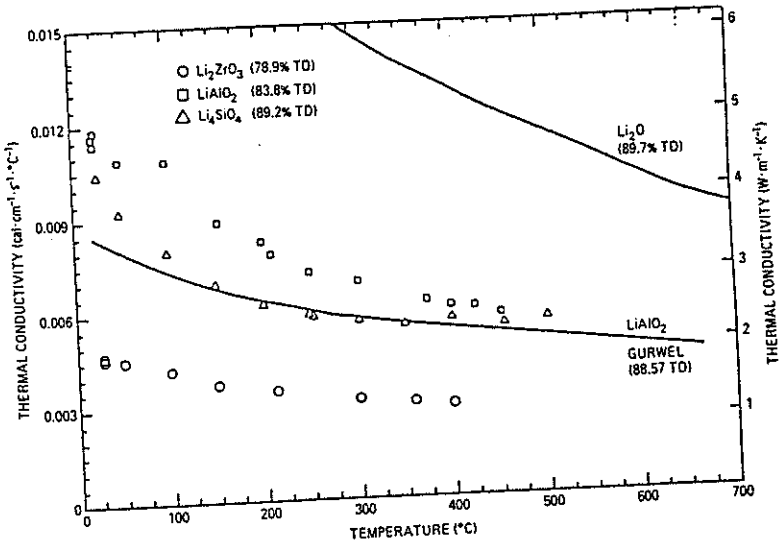

FIG. VIII-16. Thermal conductivity of $LiAlO_2$, Li_4SiO_4, Li_2ZrO_3 and Li_2O.

TABLE VIII-11. HEAT CAPACITY OF CERAMICS

Material	Heat capacity, $J \cdot kg^{-1} \cdot K^{-1}$
Li_2O	$143.9 + 1.9 \times 10^{-2} T - 4.78 \times 10^{6} T^{-2}$
$LiAlO_2$	$80.1 + 1.05 \times 10^{-2} T - 2.39 \times 10^{4} T^{-2}$
Li_4SiO_4	$53.6 + 8.32 \times 10^{-5} T + 2.29 \times 10^{5} T^{-2}$
Li_2ZrO_3	$42.8 + 1.78 \times 10^{-2} T + 2.69 \times 10^{2} T^{-2}$

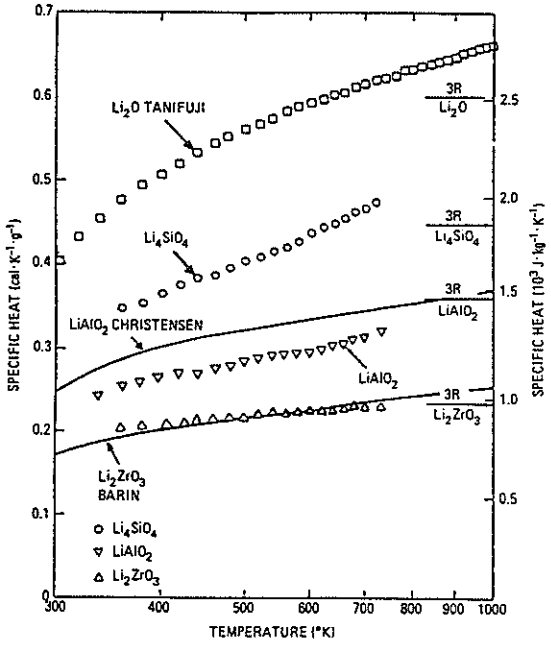

FIG. VIII-17. Specific heat of Li_2O, Li_4SiO_4, $LiAlO_2$, Li_2ZrO_3.

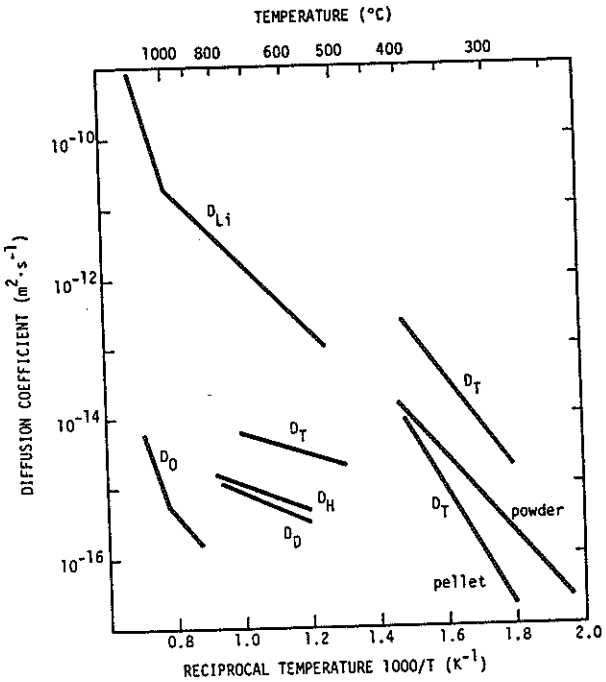

FIG. VIII-18. Diffusion coefficient for Li, O and hydrogen in Li_2O.

TABLE VIII-12. TENTATIVE VALUES FOR THE SOLUBILITY OF LiOH IN Li_2O

T, °C	ppm H_2 in He carrier gas	wt % LiOH		ppm H in Li_2O	
		cooling	re-heating	cooling	re-heating
650	500	a	a	a	a
850	65	0.0029	0.0024	1.2	1.0
950	110	0.0057	0.0053	2.4	2.2
980	500	0.0290	0.0310	12.3	13.1
990	285	0.0200	0.0120	8.4	4.9
995	40	0.0021	0.0038	0.9	1.6

[a] Moisture peaks not observed.

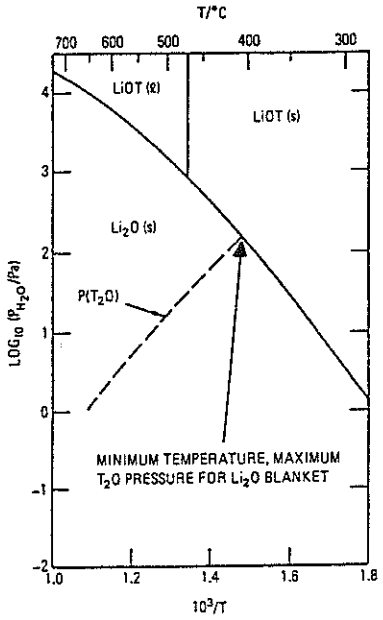

FIG. VIII-19. LiOH-Li_2O phase diagram showing operating temperature limits for Li_2O blanket.

d. Thermal expansion

Thermal expansion studies have been done for Li_2O with 75.5 – 92.5% theoretical density [4]. According to these experiments, the coefficient of thermal expansion within the 100 – 1000°C temperature range can be taken as $(33.6 \pm 0.8) \times 10^{-6}\ K^{-1}$.

e. Diffusion coefficient and tritium solubility

The lithium and oxygen self-diffusion coefficients in Li_2O are described by the following formulas [25]:

$$D_{Li} = 3.25 \times 10^{-3} \exp(-23\,400/RT)\ cm^2 \cdot s^{-1} \text{ at } T = 515–1000°C$$

$$D_{Li} = 4.06 \times 10^{3} \exp(-58\,200/RT)\ cm^2 \cdot s^{-1} \text{ at } T = 1000–1288°C$$

$$D_o = 1.52 \times 10^{3} \exp(-83300/RT)\ cm^2 \cdot s^{-1} \text{ at } T = 920–1130°C$$

where activation energies are given in $cal \cdot mol^{-1}$.

Of the greatest interest are the studies of hydrogen isotope diffusion coefficients. In Fig. VIII-18, the diffusion coefficients of hydrogen and deuterium in Li_2O, obtained in Ref. [25], are shown. These values differ considerably from those having been available up to now. Further studies in this area are needed.

The solubility of tritium in Li_2O is a key problem in determining the tritium inventory in the blanket. If chemical equilibrium is assumed for the produced tritium, it is described by the following reaction:

$$2\,LiOT\ (s) \rightleftharpoons T_2O(g) + Li_2O(s)$$

According to experimental data [25], LiOH (the same with LiOT) is practically insoluble in Li_2O. On this basis, a conclusion has been made that the total tritium inventory can be low. This is confirmed by Tetenbaum's data [5] presented in Table VIII-12.

These results allow the following conclusions to be drawn:

(1) at low temperatures the solubility of H_2O is reduced;
(2) the solubility is proportional to the H_2O concentration (pressure) in the gas phase.

f. Phase diagram for the system Li_2O-LiOH

Figure VIII-19 shows the LiOH dissociation curve corresponding to the reaction:

$$2\,LiOH(g) \rightleftharpoons Li_2O(s) + H_2O(g)$$

This curve separates a semi-plane in p-t co-ordinates, the working area of temperature and pressure being located to the left and down from the curve. So, if a pressure of 160 Pa prevails in the blanket, then at T = 410°C the separate LiOT Phase will be formed. It is also evident that whenever the blanket is cooled down, tritium will appear in the solid phase of LiOT.

g. Li_2O transport

Another important feature of Li_2O is the enhanced vaporization in the presence of moisture which can exist in the lithium zone atmosphere or can be carried in with the gas purge stream. The dependence of P_{LiOH}(gas) on temperature for various water pressures is shown in Fig. VIII-20. In the absence of water, either Li (gas) or Li_2O will be the dominating gas phase, although their pressures

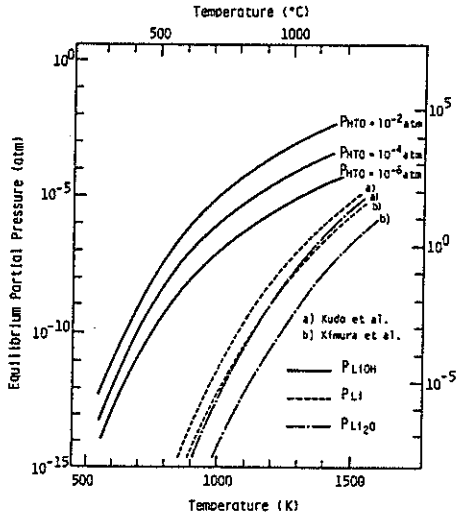

FIG. VIII-20. Equilibrium partial pressure of LiOH(g), Li(g), and Li_2O(g); total weight loss due to LiOH(g) transpiration when $V = 200\ Nm^3 \cdot h^{-1}$.

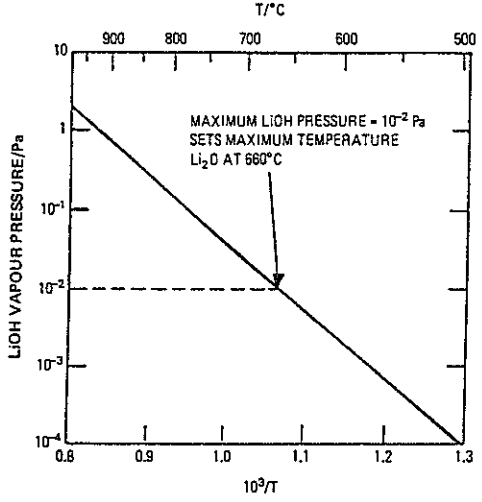

FIG. VIII-21. Vapour pressure of LiOT above Li_2O with $P(T_2O)$ equal to 1 Pa.

TABLE VIII-13. Li_2O PELLET CHARACTERISTICS

Pellet type	Conditions of sintering	Dimensions (mm) diameter	length	Bulk density (% of theor.)	Porosity (%) open	close	Surface area ($m^2 \cdot g^{-1}$)
High density	1200°C-2h	4.90	5.09	87.7–91.3	3.0	10.7	0.38
Medium density	1100°C-2h	5.07	5.45	82.3–83.2	3.4	13.0	0.57
Low density	1100°C-2h	5.32	5.46	73.2–78.1	7.6	15.9	1.3

are several orders of magnitude lower [4]. Experiments on Li_2O transport have been carried out by Tetenbaum [5] in a gas stream with a partial water pressure of about 1 Pa. The pressure of LiOT at temperatures above 900°C (Fig. VIII-21) has been shown to exceed 1 Pa, and transport of Li_2O will be substantial for pellet breeder material used in designs [5, 6, 3]. As a design criterion, the pressure of LiOT should not exceed 1% of T_2O pressure and should not be greater than 10^{-2} Pa. The temperature at which this restriction is fulfilled will be the maximum allowable temperature for the blanket. Figure VIII-21 shows that it is 660°C.

In the case of much smaller Li_2O pebbles of the design of Ref. [4], substantial Li_2O transport can be permitted. At 200 Nm^3/h gas flow rate, 10 $g \cdot h^{-1}$ water intake and 1000°C, the mass transport becomes comparable with the lithium burn-up rate (662 kg in 15 years), which is 0.6% of the starting blanket inventory (110 tons). A major part of the vaporized LiOT will condense in low-temperature (slightly above 400°C) zones.

h. Pellet fabrication and preparation

Li_2O pellets can be produced either by sintering or by hot pressing. The purity and the microstructure of the pellets are quite sensitive to minor variations in the fabrication procedures. Sintering in vacuum at 1000°C for 4 h resulted in large weight loss of the pellet. However, sintering temperatures may be much lower (possibly as low as 450°C) if significant amounts of LiOH are present [5]. The characteristics of pellets sintered in vacuum are shown in Table VIII-13 [3].

The kinetics of sintering have been analysed in detail in Ref. [6].

i. Chemical properties

Li_2O is very hygroscopic, reacting readily with moisture to form LiOH. This feature imposes very strict requirements on the handling and storing procedures, taking into account the fact that moisture absorption takes place even at room temperature. Li_2O also reacts with CO_2 in air to form Li_2CO_3. Reacting with a large number of metal oxides it forms ternary oxides, e.g. $LiCrO_2$. Thus, samples of Li_2O prepared without the utmost care necessary are likely to contain significant quantities of LiOH, Li_2CO_3, etc. Commercially available material appears to have at least 2% weight of both LiOH and Li_2CO_3. Careful laboratory preparations have achieved rather pure material with 0.25% weight of Li_2CO_3 and <0.1% weight of LiOH [5].

4.1.2. Radiation effects

The stability of Li_2O pellet microstructure in the anticipated thermal and radiation environment is a major concern. The chemical effects produced by burn-up of lithium and displacement damage effects could cause enhanced sintering which would lead to pore closure and a build-up of T or LiOT inventory. A maximum temperature of 0.6 T_m, which corresponds to about 750°C for Li_2O has been suggested but experimental information is required to determine the operating temperature limits.

Experimental results on studying 70% dense Li_2O samples are presented in Ref. [5]. They were irradiated to fluences of $\approx 2 \times 10^{21}$ n·cm^{-2} at temperatures of 750, 850 and 1000°C. Post-irradiation examination revealed that the pores became completely closed in samples irradiated at 850 and 1000°C and significant changes in microstructure at 750°C were observed. These results indicate that Li_2O must be operated at temperatures considerably below 750°C if the desired open microstructure is to be stable. A maximum temperature of 650–700°C is considered on the basis of radiation effects. Obviously, additional experimental investigations are required to more accurately determine the temperature limits.

4.1.3. Tritium recovery

a. Analysis of T_2O transport

The microstructure effects upon T_2O percolation in Li_2O were studied [1]. It was supposed that a pellet consists of pressed or sintered product with a tailored bimodal pore distribution, i.e. a small grain size (<1 μm) and a fine porosity within larger particles (≈1 mm diameter) with a more coarse porosity between particles. Li_2O is perforated with ≈2 mm diameter holes through which low-pressure (≈0.1 MPa) helium is purged to recover the tritium from the breeder.

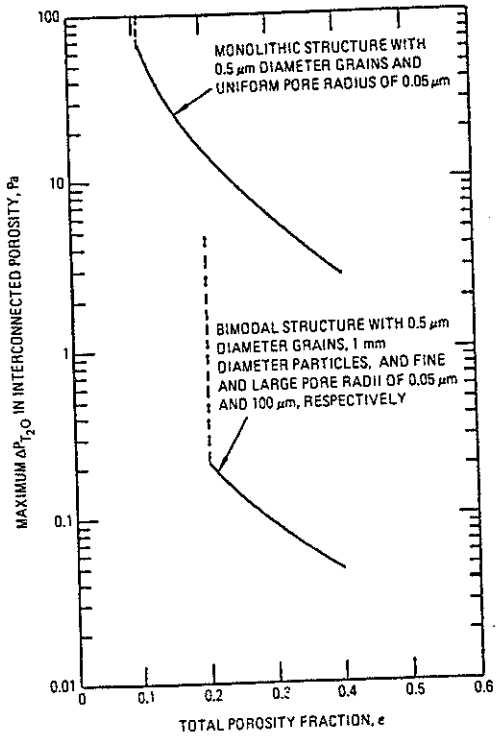

FIG. VIII-22. Increase in T_2O partial pressure from the helium purge stream to the outer radius of a unit blanket cell as a function of total porosity fraction and pore distribution (monolithic versus bimodal).

Tritium generated within the grains has to diffuse to the surface of the grains, desorb as T_2O and migrate (percolate) through the interconnected porosity to the helium purge stream where it is transported to the tritium processing system. The T_2O pressure in the 2 mm holes was supposed to be approximately 1 Pa. In regions located at some distance from these holes the partial pressure of tritium was estimated to be about 150 Pa. The pressure rise was considerably less for the breeder microstructural configuration having a bimodal pore distribution (Fig. VIII-22).

b. Tritium inventory

In the absence of radiation effects, the tritium inventory is assumed to be the sum of 'adsorbed', 'diffusive' and 'solubility' inventories. An estimation of the adsorbed inventory was reported in Ref. [6]. The inventory results from adsorption of T_2O (g) on the Li_2O surface mostly at low temperature in the range of 400–500°C. The total T_2O adsorption inventory amounts to a considerable quantity of as much as 270 g.

The total diffusive inventory was estimated [5] to be about 20 g, over 80% of which is also concentrated in the regions of lowest temperature (below 470°C).

The solubility inventory was extrapolated [5] from the results obtained by Tetenbaum to 7×10^{-3} wppm of tritium at 410°C and 0.12 wppm at 650°C for T_2O pressure of 1 Pa. This translates to a solubility inventory of about 5 g. Thus, in the absence of radiation effects, the total tritium inventory in the blanket is estimated to be about 300 g.

Radiation effects, sintering and trapping can significantly increase the tritium inventory. Even restructuring grain growth represented by a threefold increase in grain size would increase the diffusive inventory by an order of magnitude up to 200 g. Although the degree of radiation-induced tritium trapping is highly uncertain, estimates based on results from ion bombardment studies indicate that high tritium concentrations may occur.

In case of a breeder temperature above 700°C, an unacceptably high inventory of several kilograms is supposed to exist. Effects are lower in the temperature range of 400–650°C, and the tritium inventory may stay on the level of 1 kg.

c. Design requirements

Two designs will be considered below. The first is based on the INTOR reference design [2] using solid breeder in the form of Li_2O pellets and H_2O in tubes. The second represents pebble-type Li_2O elements operating at a higher temperature level [4]. The main operating conditions are shown in Table VIII-14.

d. Tritium release

Experimental data on gas release from Li_2O pellets were presented in Ref. [4]. The initial pellet composition included: Li_2O - base, LiOH - 3.43–2.25%; and Li_2CO_3 - 0.5%. Pellets were irradiated in the JRR-4 reactor with 4.5×10^{13} $cm^{-2} \cdot s^{-1}$ thermal neutron flux. Table VIII-15 lists the composition of gases released from neutron-irradiated Li_2O pellets heated stepwise up to 1070 K in vacuum.

It is considered that HTO(g) release from the sintered Li_2O pellet is determined by the diffusion of tritium in the grain. The diffusion coefficient for the Li_2O pellet with an average grain radius of about 5 μm can be expressed as

TABLE VIII-14. Li_2O BLANKET PARAMETERS

Option Type of breeder element	1 pellet	2 pebble
Upper operating temperature for Li_2O (°C)	650	1000
Lower operating temperature for Li_2O (°C)	400	400
Coolant inlet temperature (°C)	50	50
Coolant outlet temperature (°C)	100	90
Coolant pressure (MPa)	4.0	1.0
Neutron heating rate near first wall ($W \cdot cm^{-1}$)	20	9.0
near reflector/shield	0.4	0.3
Tritium generation rate ($g \cdot s^{-1}$)	5×10^{-4}	5×10^{-4}
Purge stream T_2O pressure (Pa)	1.0	3.2
Purge stream LiOT pressure (Pa)	10^{-2}	10^{-6} at 400°C
Purge stream pressure (MPa)	0.1	0.1
Purge stream flow rate (total) ($L \cdot s^{-1}$)	–	56
Purge stream velocity ($m \cdot s^{-1}$)	–	0.006
Purge stream volume (L)	–	30 000

$D = 59.6 \exp(-36\,900/RT)$ $cm^2 \cdot s^{-1}$, up to a density of 89% from the theoretical one. Experiments on tritium release from Li_2ZrO_3 and Li_2TiO_3 are described in Ref. [25].

e. Kinetics of LiOT

As was shown above, at high temperatures, Li_2O reacts with water vapour to form LiOH(g)/LiOT(g), which causes condensation of solid LiOH(s)/LiOT(s) in the low-temperature zone. LiOT pressure in the blanket depends on the equilibrium maintained by the He temperature and the partial pressure of T_2O; and the pressure of LiOT over Li_2O will be low ($\approx 10^{-11}$ atm at 400°C) at low temperatures. Then it is possible that the amount of LiOT condensing on the structural material surfaces will be small.

TABLE VIII-15. COMPOSITION OF GASES RELEASED FROM NEUTRON-IRRADIATED SINTERED Li_2O PELLETS (76.5% TD) HEATED UP TO 1070 K

Material	Neutron fluence (cm^{-2})	Gas distribution HTO	HT	CH_3T	C_2H_{2n-1} ($n=1,2..$)	retention
Li_2O pellet[a]	5.4×10^{15}	97.8	1.4	0.6	0.01	0.2
Li_2O pellet[b]	5.4×10^{15}	95.4	3.5	0.5	0.03	0.6
Li_2O powder	5.4×10^{15}	99.1	0.4	0.1	0.2	0.2

[a] As received.
[b] Heated at 770 K for 1 h and at 970 K for 2 h under vacuum before irradiation.

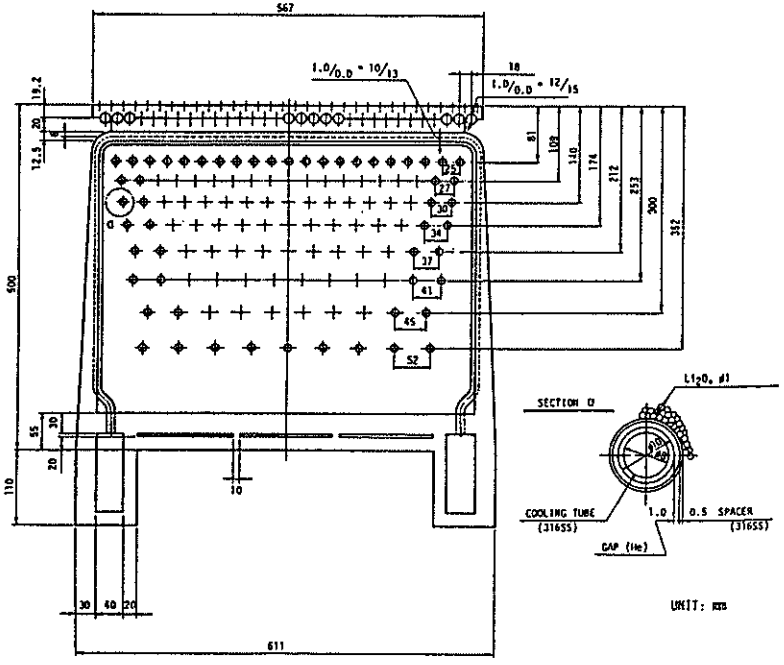

FIG. VIII-23. Cross-section of tritium-producing blanket (T_{min}/T_{max} = 450/700°C).

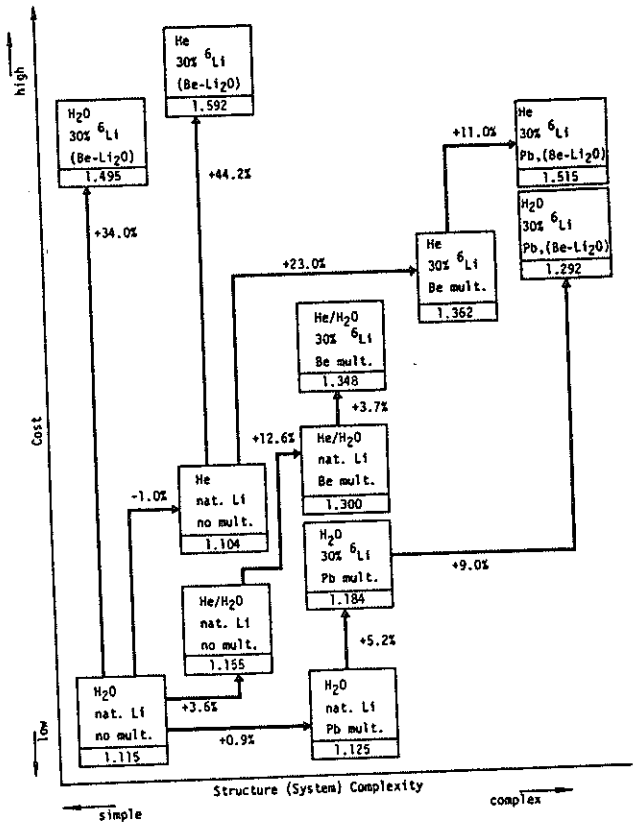

FIG. VIII-24. Relation of tritium breeding ratio improvement with structure complexity and cost.

4.1.4. *Blanket design*

INTOR reference and alternative blanket designs [4–6] were developed. In Ref. [4], the concept of a blanket design with the Li_2O breeder outside the cooling tubes was considered. The coolant tubes shown in Fig. VIII-23 are arranged according to the nuclear heating rate. The breeder which consists of small pebbles of natural Li_2O is packed in the blanket vessel. A diameter of 1 mm was chosen for the pebbles in order to reduce the wall effect of the coolant tubes.

A helium gas gap is provided around the coolant tubes in the breeder zone in order to control the minimum temperature of Li_2O.

Neutronic studies of this design with lead and beryllium multipliers were carried out. The relation of tritium breeding ratio to cost and structural complexity is shown in Fig. VIII-24.

4.1.5. Methods of accommodating power variations in the blanket

a. Active methods

Previous studies of solid breeder blankets have identified two active methods for breeder temperature control: (1) changing thermal conductance of the breeder-to-tube interface; (2) changing coolant temperatures.

Changes in thermal conductance at the breeder/tube interface of several orders of magnitude can be effected for a small-width helium gap by varying the pressure of the helium within the range of $10^{-1} - 10$ Pa. Outside this range, large order-of-magnitude pressure changes have little effect on the thermal conductance across the gap.

Coolant temperature changes can be used to accommodate reactor power changes up to 20% if a breeder temperature between 400°C and 650°C has to be supported.

It was agreed that these methods can be used to accommodate power density variations of up to ±33% from the nominal design value (i.e. power change factor F = 2, where F = maximum power/minimum power).

b. Passive methods

Since temperature limits are imposed on the Li_2O breeder, the only design change considered viable to accommodate power changes is to reduce the allowable breeder cylinder outer radius, which, in the end, reduces the blanket tritium breeding ratio.

TABLE VIII-16. SENSITIVITY ANALYSIS FOR BREEDER TEMPERATURE (Li_2O)

Sensitivity to heating rate	+4°C/%
Sensitivity to tube arrangement	+40°C/1 mm
Sensitivity to effective thermal conductivity:	
to packing fraction of Li_2O pebbles	+8°C/%
to thermal conductivity of Li_2O	+2°C/%

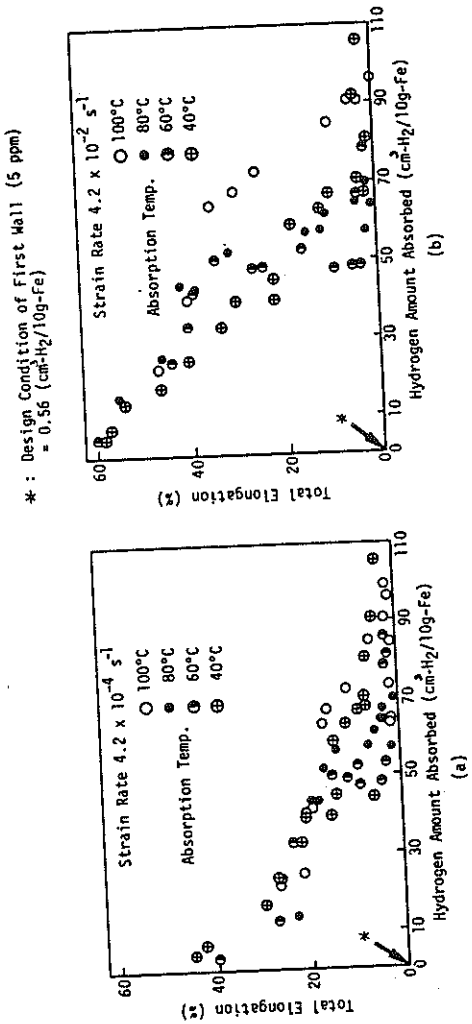

FIG. VIII-25. Effect of hydrogen amount absorbed on total elongation [3].

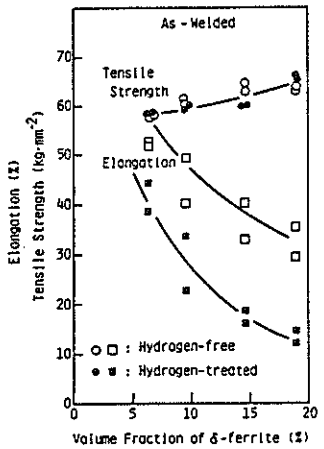

FIG. VIII-26. Effect of δ-ferrite on hydrogen embrittlement of As-welded material [7].

The tritium breeding ratio for one of the possible blanket design solutions [5] decreases to the value of 0.08 with F changing from 1 to 2.

A sensitivity analysis carried out in Ref. [4] for the breeder (Li_2O), the temperature of which is controlled by the coolant tube arrangement and the thermal resistance layers around the tube, permits the changes in the nominal parameters to be evaluated on the basis of data given in Table VIII-16.

The following conclusions can be drawn:

- breeder material with higher thermal conductivity should be used in blanket design. Li_2O seems to be the best candidate material;
- further study is needed to verify the sufficiency of the estimated 50% margin in power variation.

4.1.6. Hydrogen influence on weldability

In the first wall of a nuclear fusion reactor, tritium is absorbed into the austenitic stainless steel such as 316 SS which is one of the candidate structural materials. This absorbed tritium will be around five ppm in weight, at most.

The general characteristics of hydrogen embrittlement of austenitic stainless steel will be described below. From the characteristics, ductility, one of the key factors in weldability, is not appreciably affected by the hydrogen amount around five ppm in weight, as is shown in Fig. VIII-25. It is certain that δ-ferrite in the

weld metal of austenitic stainless steel decreases the ductility, as is shown in Fig. VIII-26. However, the amount of hydrogen absorbed in these figures is not clear. Therefore, it is necessary to clarify the effect of δ-ferrite on the ductility under a hydrogen amount of about five ppm in weight. Further, it should be ascertained whether tritium has other serious effects on the austenitic stainless steel or not. From these considerations, a proper welding process must be chosen in first-wall repair work. A more detailed discussion is presented in Ref. [4].

4.2. Liquid breeders

Liquid breeder investigation has been focused on the eutectic $Li_{17}Pb_{83}$. New information was sought on the basic properties of this material, together with a revision and up-dating of the blanket design concepts developed during the previous period.

4.2.1. Data base

The preparation of the alloy is currently carried out on a laboratory scale. A typical chemical analysis of the alloy prepared is: 99.23 wt% Pb, 0.68 wt% Li, 0.001 wt% N, 0.002 wt% Fe.

4.2.1.1. Physical and chemical properties

The data now available on the physical properties of $Li_{17}Pb_{83}$ are summarized in Table VIII-17. Melting temperature and enthalpy of fusion have been recently measured by Reiter et al. [18]. Specific heat at constant pressure and entropy differences have been calculated from these measurements. Vapour pressure and thermal conductivity have been calculated by using the experimental data on Li and Pb. The solubility of hydrogen isotopes in liquid $Li_{17}Pb_{83}$ has been studied recently by Pierini et al. [16], Veleckis [17] and Wu and Blair [19]. The main results of these studies are presented in Table VIII-18. The differences of these results call for further measurements, mainly in the pressure range 100–200 mbar and in the temperature range from the melting point to 600°C.

The only information on hydrogen diffusion rates in $Li_{17}Pb_{83}$ comes from Pierini et al. [16], who deduced a diffusion rate, at 673 K, of about 10^{-4} $cm^2 \cdot s^{-1}$ from the time slope of solubility measurements.

4.2.1.2. Compatibility with structural materials

Critical compatibility issues for $Li_{17}Pb_{83}$ with structural material are of two types: (a) corrosion mass transport, (b) effects on the mechanical integrity of the structure.

TABLE VIII-17. PHYSICAL PROPERTIES OF $Li_{17}Pb_{83}$

Property	Unit		T (°C)	Remarks
Molecular weight	$g \cdot mol^{-1}$		173.2	
Density	$g \cdot cm^{-3}$	300	9.51	
		400	9.43	
Thermal expansion coefficient	K^{-1}		8×10^{-5}	
Lithium content	$g \cdot cm^{-3}$		0.066	
Melting temperature	°C		234.7	
Enthalpy of fusion	$J \cdot g^{-1}$		29.59	
Specific heat	$J \cdot g^{-1} \cdot K^{-1}$			
(at constant pressure)	solid	234.7	0.195	
	liquid	234.7	0.250	
		300	0.158	
Enthalpy difference	$J \cdot g^{-1}$		–	
	solid	234.7	34.40	
	liquid	234.7	63.99	
		300	77.45	
Entropy difference	$J \cdot g^{-1}$			
	solid	234.7	0.084	
	liquid	234.7	0.142	
		300	0.167	
Vapour pressure	torr	300	1.3×10^{-7}	calculated from Li
		400	1.7×10^{-5}	and Pb data
Thermal conductivity	$W \cdot cm^{-1} \cdot K^{-1}$			
		300	0.20	calculated from Li
		400	0.22	and Pb data
Heat of reaction:	$KJ \cdot g^{-1}$			
with water			19.1	
with air			31.6	
Activation energy	$kcal \cdot mol^{-1}$	200–400	24	
Heat of reaction with water	$KJ \cdot g^{-1}$		19.1	

A series of compatibility experiments between pure $Li_{17}Pb_{83}$ and steel has been carried out by Coen et al. [20]. They consist of:

(a) static corrosion tests in the temperature range 400–600°C up to 6000 h;
(b) tensile tests on notched specimens treated at 350°C under constant load and for times up to 1000 h.

TABLE VIII-18. SOLUBILITY OF HYDROGEN ISOTOPES IN $Li_{17}Pb_{83}$

Isotope	Temperature (K)	Pressure range (mbar)	Sieverts constant ($bar^{1/2} \times 10^3$)	Ref.
H	623	200–1000	0.8	[16]
H	673	200–1000	1	[16]
H	773	200–1000	2.6	[16]
H	700–900	5–130	(7.1 ± 1.5)	[17]
D	850–1040	0.01–0.1	5.0	[19]
T	515	0.21	7.25	[19]
T	515	14	6.52	[19]
T	515	21.3	3.70	[19]

TABLE VIII-19. CHEMICAL COMPOSITION OF STEELS (Polzunov Institute experiments)

Type	Element content (%)								
	C	Si	Mn	Cr	Ni	Mo	Cu	Ti	V
08X14MΦ	0.08	0.33	1.1	14.0	–	0.32	0.1	–	0.25
07X13AГ20	0.06	0.57	22.0	13.6	0.21	0.06	0.13	0.01	–
09X16H15MБ	0.07	0.4	0.38	15.8	14.7	2.76	–	–	–

The steel tested was an AISI 316L (solution annealed) furnished in the form of 20-mm-diam. rods. No corrosion was found at 400°C. At 450°C, after 3000 h, a small corrosion layer (≅ 10 μm) was observed. The corrosion becomes significant at 500°C. The corrosion mechanism is identical in all cases; it follows the same pattern as the corrosion by liquid lithium or lead, i.e. there is a strong nickel depletion and the structure of the affected zone is no longer austenitic. Lead and lithium penetration in the matrix is also evident. The tests at 350°C on the notched specimen under a constant uniaxial tensile load of 140 MPa showed that, after 500 h, some microcracks appeared at the tip of the notch. After treatment in the same conditions for 1000 h, the number of microcracks increased, and it seemed that a principal crack had developed. In both cases, no corrosion layer was noticed

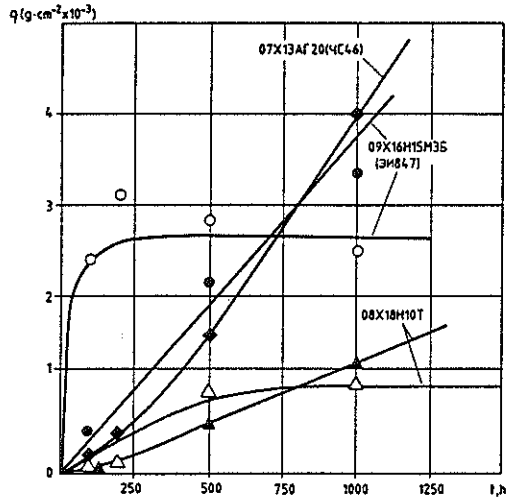

FIG. VIII-27. Specific weight loss for steels 0Х18Н10Т, 09Х16Н15М3Б (ЭИ 847), 07Х13АГ20 (ЧС 46) versus exposure to Pb-Li eutectic: a) dynamic conditions (●, ▲, ♦); b) static conditions (○, △, ◇).

in the entire specimen but lead penetration in the cracks had become evident. Most probably, also lithium was present. Similar measurements with other liquid metals (lead, bismuth and lead-bismuth eutectic) [5] show severe loss of ductility and reduction of the fatigue strength of steels.

An extensive series of corrosion tests of structural materials on $Li_{17}Pb_{83}$, both under static and dynamic conditions, has recently been carried out at the Polzunov Central Boiler-Turbine Institute of Leningrad [6]. A large number of steels have been investigated: (a) ferritic steels, (b) Ni-Cr and Mn-Cr austenitic steels, and (c) Ni-base alloys.

The composition of three of these steels is given in Table VIII-19.

In the dynamic tests (natural convection, breeder velocity 0.18 $m \cdot s^{-1}$), the temperature of the samples (rods 7 mm in diameter) was 430°C. The static experiments were carried out at 430°C. The maximum exposure time was 1500 h. The corrosion effects were evaluated by measuring the weight losses and by metallographic tests. The main results are as follows:

(a) The ferritic type of steels did not show any appreciable loss of weight, even after maximum exposure;

TABLE VIII-20. WEIGHT LOSSES ($g \cdot cm^{-2}$) OF STEELS

Type	10^4 h	10^5 h
08Х14МФ	9.0×10^{-4}	2.5×10^{-3}
07Х13АГ20	5.5×10^{-2}	0.7
09Х16Н15М3Б	2.5×10^{-2}	0.2

(b) the Ni-Cr steels gave evidence of a sensible corrosion in dynamic tests, as a result of continuous thermal mass transfer, linear in time. In static tests a saturation of the corrosion effects was noted (Fig. VIII-27);
(c) a similar trend was observed for the Mn-Cr steels.

The extrapolated specific weight losses for these steels under dynamic conditions up to 10^5 h is presented in Table VIII-20. For Ni-base alloys the corrosion effects were much more important.

Preliminary results of static capsule tests with AISI-316 steel and ferritic steel (HT-9) at 500°C performed in the USA have been reported [5]. They indicate much higher (about 100 times) corrosion rates in $Li_{17}Pb_{83}$ as compared to Li in the same conditions.

Initial conclusions can be drawn from these experiments:

(a) corrosion rates of austenitic steels at temperatures higher than 450°C are possibly excessive;
(b) ferritic steels, in this respect, exhibit a better behaviour which should permit the maximum allowable temperature to be increased;
(c) liquid-metal embrittlement and other mechanical integrity effects at low temperature (250–350°C) could pose a problem.

4.2.1.3. Chemical reactivity

A number of experiments studying the chemical reactivity of $Li_{17}Pb_{83}$ with air, water and structural materials have been carried out at JRC-Ispra [3]. The following phenomena were investigated:

(a) Self-ignition:
The alloy was placed in an open crucible and heated from beneath with a gas flame. At a temperature of 300–400°C, a grey oxide layer was formed on the surface. When continuing the heating up to 500°C and higher, this layer

showed the yellow-red colouring of PbO. It was impossible to cause self-ignition of the samples, even though the oxide layer was disturbed by stirring.

(b) Reactions with contact materials:
Samples of the eutectic were placed in open crucibles of different materials and heated from above with a torch. The sample in a stainless-steel crucible spread rapidly over the whole bottom of the crucible and local non-propagating burning occurred, which appeared to cease as the lithium burned out. The reaction in a quartz crucible was slower. The alloy placed in a crucible of insulating material was the last to react. For comparison, the same experiment was conducted with samples of pure lithium. It appeared that the reactions of the eutectic are harmless, compared with the violent reactions of lithium, especially in the case of insulating material.

(c) Reactions with water:
An experiment in which the $Li_{17}Pb_{83}$ alloy at 350°C was added slowly to water at ambient temperature did not exhibit any significant hydrogen generation. This experiment was repeated in a closed stainless-steel crucible in order to show whether hydrogen was formed. A controlling experiment with pure lithium showed a pressure increase exactly corresponding to the hydrogen formation due to a total lithium-water reaction. Conversely, in the test with $Li_{17}Pb_{83}$, the pressure increase corresponded to a reaction of about 16% of the alloyed lithium.

In similar experiments carried out at Argonne National Laboratory [5] in which the alloy was heated to 500°C and then dropped into water at 90°C, minimal evidence of a chemical reaction was observed. Also, measurements of Sabougi et al. [5] showed that the lithium activity in $Li_{17}Pb_{83}$ was about 1×10^{-3}, which is three orders of magnitude lower than that of pure lithium.

Measurements of the reactivity of $Li_{17}Pb_{83}$ with water and air have also been performed in the USSR [6], with similar trends as in the European and American experiments.

According to these results, it may be concluded that the chemical reactivity of $Li_{17}Pb_{83}$ with air and water is low. The behaviour can, however, be different if the molten mass is fragmented or the water is forcefully injected into the melt, as might have been the case in a loss-of-coolant accident. Experiments undertaken to investigate the hydrodynamic and pressure effects in these conditions are in progress [3].

4.2.2. Design aspects

The conceptual designs developed during Phase One have been revised and detailed [3], using the new basic data. The first wall is constituted by a series of tubes, facing the plasma and separated from the blanket units, as shown in Fig. VIII-28. The breeding blanket consists of vessel units, cooled by pressurized

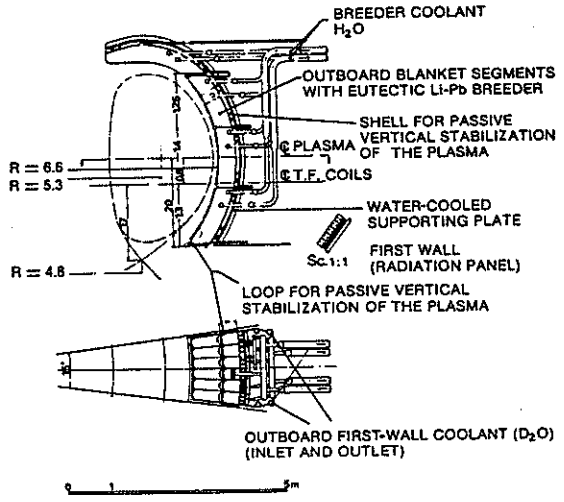

FIG. VIII-28. INTOR elevation view with liquid breeder ($Li_{17}Pb_{83}$) blanket.

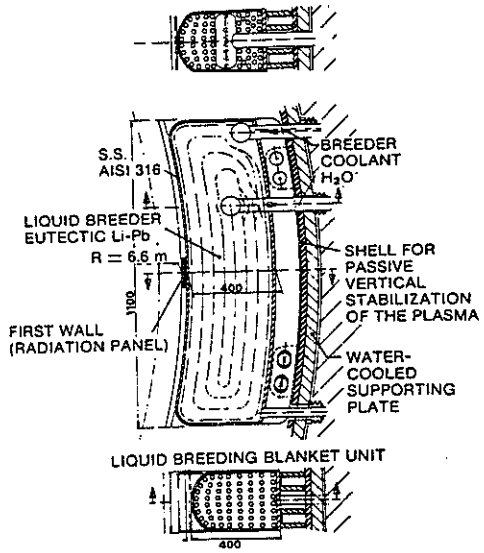

FIG. VIII-29. Liquid breeder ($Li_{17}Pb_{83}$) blanket unit.

TABLE VIII-21. $Li_{17}Pb_{83}$ – INTOR BLANKET PARAMETERS

Type	vessel units
Arrangement	poloidal
No. of units in a segment	30
Size	rectangular with circular shape in front of plasma
Coolant in tubes	H_2O
Tube ID/OD, mm	18/21
Coolant temp., °C	240–260
Coolant press., MPa	5.0
Breeder thickn., cm	45
Max. struct. temp., °C	370
Max. breeder temp., °C	350
Max. stress, MPa	30
Local tritium breeder ratio	1.20
Net tritium breeding ratio	0.72

H_2O, arranged along the poloidal direction. The blanket is located inside the main vacuum vessel of the machine and is subdivided into 24 segments. One of them is formed of units along the toroidal direction and of units along the poloidal one. For each segment, a single inlet/outlet cooling circuit is foreseen, collecting the cooling tubes in the blanket units arranged as shown in Fig. VIII-29. The $Li_{17}Pb_{83}$ is circulating at low speed through a separate circuit towards the outside for continuous tritium removal.

The design parameters of the breeder unit, shown in Table VIII-21, result from a compromise between various requirements:

- the minimum temperature and pressure of the blanket coolant is determined by the need of maintaining $Li_{17}Pb_{83}$ always liquid during the reactor operation;
- the thickness of the vessel unit is determined by the safety requirements in case of rupture of a cooling tube;
- the maximum temperature of the breeder must not exceed 400°C in order to avoid possible corrosion with the stainless-steel structures.

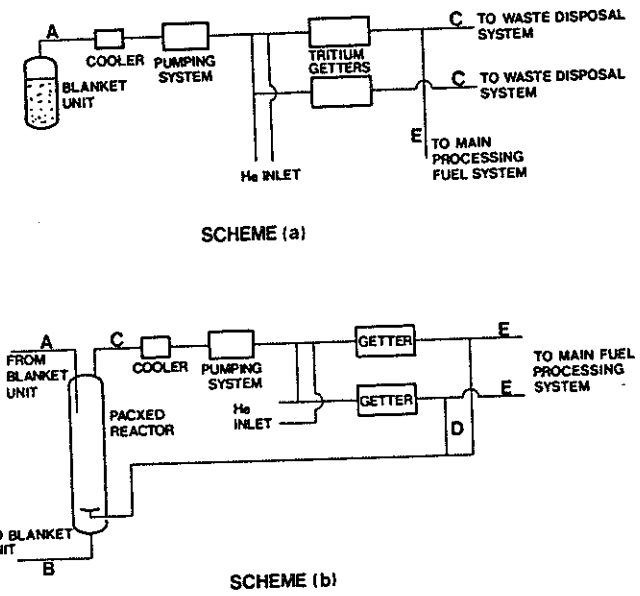

FIG. VIII-30. Tritium recovery schemes from liquid breeder ($Li_{17}Pb_{83}$) blanket:
(a) direct pumping scheme
(b) countercurrent inert-gas flushing scheme

4.2.2.1. Tritium recovery and permeation into coolant

Two schemes for tritium recovery from the blanket have been worked out [3] (Fig. VIII-30):

(a) direct pumping of tritium above the breeder in the blanket unit;
(b) countercurrent inert gas flushing scheme.

In the second scheme, which is more attractive, $L_{17}Pb_{83}$ is circulated at low speed (few $cm \cdot s^{-1}$), and the tritium is extracted in a packed column outside the blanket unit in countercurrent into an inert gas (helium). A tritium inventory of 200 g can be maintained in the blanket by using an extraction column of 1.7 m height and 0.15 m diameter and a helium flow rate of about 9.0 $L \cdot s^{-1}$ at 400°C, if the entire quantity of the breeder is extracted from the container, purified and recycled in one day.

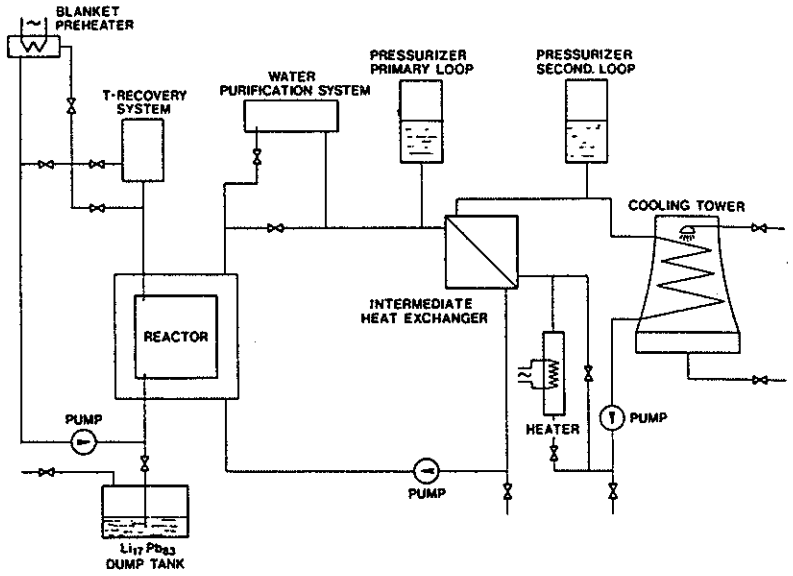

FIG. VIII-31. Layout of the plant circuits ($Li_{17}Pb_{83}$ blanket).

The tritium permeation through the cooling structures of the blanket units is comparable to that expected into the coolant of the first wall (0.1–0.2 g per day). Means to reduce this permeation could be envisaged. A water detritiation system similar for the two coolant circuits has to be provided.

4.2.2.2. Pre-heating systems

A layout of the facility to keep the breeder always liquid during the reactor operation has been studied [3] (Fig. VIII-31). Before start-up, the breeding material is pumped into the assembled blanket vessels in liquid phase. The tubes of the liquid-metal systems are equipped with external electric trace heaters fixed in longitudinal direction on the outer walls. This pre-heating method has already proven its reliability in radioactive liquid-metal systems (Phenix fast breeder reactor). The blanket vessels, being placed near the plasma, cannot be equipped with external heaters. The pre-heating of that part of the structure is done from inside by hot gas circulating in the space provided for the liquid metal.

The heating up of the primary and secondary cooling loops is realized by an electric heater installed in a bypass of the secondary loop.

As a conclusion, we may say that the problem of keeping the breeder liquid during the reactor operation does not seem to represent a critical issue for the use of $Li_{17}Pb_{83}$ in the reactor.

4.2.3. Conclusions

Breeding blanket concepts using $Li_{17}Pb_{83}$ suited to produce about 70% of the tritium burned in INTOR have been developed and look workable; however, to confirm their feasibility, further experimental information is required on:

(a) physical and chemical properties, mainly for tritium recovery;
(b) compatibility between breeder and structural material (corrosion/mass transfer and embrittlement effects);
(c) effects of breeder-coolant (water) interaction.

5. TRITIUM SYSTEM

5.1. Introduction

The INTOR tritium system (Fig. VIII-32) is composed of all the subsystems of the device that have to process gases or liquids containing tritium in the form of T_2 or T_2O. The different parts are then the following:

- plasma exhaust reprocessing system (P.E.R.S.)
- neutral beam reprocessing system (N.B.S.)
- blanket exhaust processing system (considering the reference INTOR blanket with Li_2O as breeding material, as described in Section 2) (B.R.S.)
- gaseous waste processing system (G.W.P.S.)
- atmosphere processing systems (E.C.S.[1])
- coolant reprocessing system (C.R.S.).

Each of these subsystems must fulfil different functions and, for some of them, different solutions are available, but there is always an impact on the tritium inventory and the tritium contamination. The system to be described hereafter is only an illustration intended to give an idea of the system complexity. The solutions obtained seem to be the most reasonable ones, with today's knowledge, but some choices will certainly change when the R and D programme has been accomplished.

[1] ECS stands for Emergency Air Cleaning System.

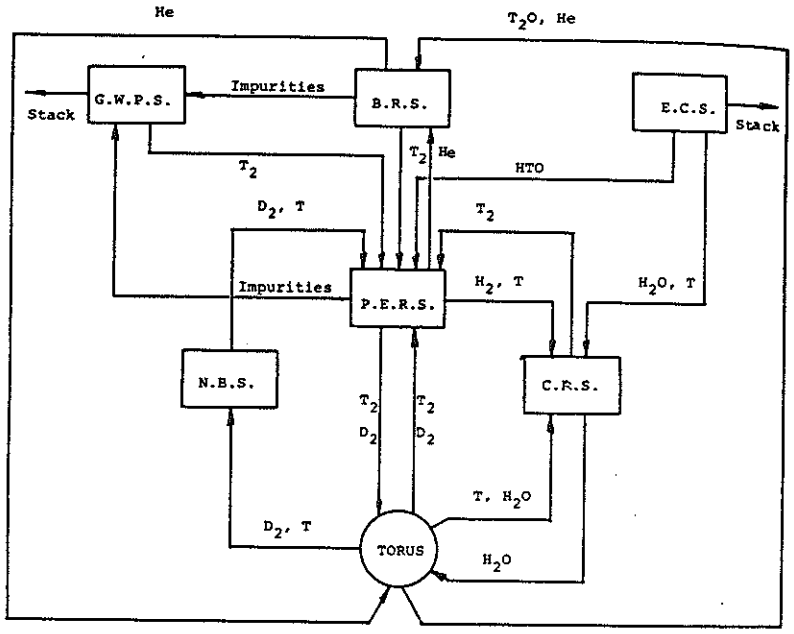

FIG. VIII-32. Interconnections inside the tritium system.

5.2. Plasma reprocessing system

The torus and neutral-beam vacuum system is the source term for the plasma exhaust reprocessing system.

All lines coming from the torus are connected before going through cold traps in which impurities are solidified and sent, after trap regeneration, to the waste processing line (other methods like palladium-silver membranes or getters may also be used).

At a temperature of 35 K, H, D, T and He are in a gaseous form, whereas impurities are in solid form. Then, the processed gas is sent to the falling-film condensor in which H, D, T only are liquefied. The gaseous helium upstream is sent to the blanket processing line, while the liquid tritium-deuterium flow is sent to the isotopic separation system. This system includes five interconnected cryodistillation columns.

TABLE VIII-22. MASS FLOW RATES – PROCESSED GASES

Plasma	
tritium exhausted ($g \cdot d^{-1}$)	1.470
deuterium exhausted ($g \cdot d^{-1}$)	977
Neutral injectors:	
deuterium pumped ($g \cdot d^{-1}$)	276
tritium pumped ($g \cdot d^{-1}$)	1
Gases composition to process	
Plasma exhaust ($g \cdot mol \cdot h^{-1}$)	T_2 : 10.2 D_2 : 10.2 He : 1.07
Total molar flow rate ($g \cdot mol \cdot h^{-1}$)	21.47
Neutral injectors ($g \cdot mol \cdot h^{-1}$)	D_2 : 2.875 T_2 : 0.007
Total molar flow rate ($mol \cdot h^{-1}$)	2.882

Three bottom flows for DT, D_2 and T_2 are driven to the neutral injectors and torus feed processing line. The plasma exhaust isotopic separation columns system is interconnected with the cryodistillation column of the primary coolant and the detritiation system electrolysis cell of the blanket processing system, allowing, in this way, a complete autonomy of the tritium-handling system.

Considering the different scenarios foreseen for INTOR, the plant must be able to accommodate the highest possible flow rate so we chose the highest values of performance, relative to the Stages II and III for the plasma and to Stage I for the neutral injectors.

The mass flow rates given in the Phase-One report are given in Table VIII-22.

5.3. Breeding tritium processing system

The reference breeding material is Li_2O, working in the temperature window 400–650°C, but higher temperatures may be used (see Section 4). Tritium formed inside the breeder may be recovered, by using helium as a sweeping gas. INTOR specifications stipulate a breeding ratio equal to 0.6, which corresponds, during Stages II and III of INTOR, to a tritium production of 50 g per day.

The tritium recovering process from the blanket may be as follows:

Helium leaves the blanket at a temperature less than 600°C, which could be too high to be compatible with the compressor; so the first step of the process is to cool this gas down to a temperature compatible with the compressor material. This cooling is achieved in a countercurrent heat exchanger with helium entering inside the blanket. Tritium leaves the blanket mainly as T_2O but a small fraction is in the form of T_2; so the following step consists of converting this fraction into tritiated water on a catalytic bed, working at 200°C. The efficiency of such a reaction is higher than 99.99%, so the hypothesis that helium leaving the catalytic bed contains only water is reasonable. After this step, helium is cooled down to liquid nitrogen temperature to trap water as frost and to decrease the partial vapour pressure below 10^{-4} Pa, giving a very good recovery efficiency. Leaving the cold trap, helium is heated again up to 400°C before re-entering the blanket.

The trapped water fraction is recovered, from time to time, by heating up the vessel to room temperature, with the aim of recovering tritiated water in liquid form. This water is directed to an electrolysis cell where the decomposition occurs. The oxygen flow is sent back to the catalytic bed. The tritium flow is directed to the purification of the fuel exhaust processing line.

For the reference design (Li_2O pellets) the T_2O partial pressure above the breeding material is of the order of 1 Pa in equilibrium conditions, considering the temperature window. With the aim of keeping a concentration-driving gradient, work with a T_2O partial pressure around 0.1 Pa inside the helium sweeping gas was devised. If, in addition, it is foreseen to recover daily all the tritium bred, i.e. 50 g, the corresponding helium flow rate would be 7800 $m^3 \cdot h^{-1}$. Considering the magnitude of the helium flow rate, it appears reasonable to subdivide the total flow into twelve INTOR segments, i.e. 650 $m^3 \cdot h^{-1}$ per segment. Handling this even large flow leads to an increase in the outside working pressure up to 1 MPa, with the aim of decreasing the dimensions of the different circuit vessels.

The assumption of a driving force of 1 Pa to 0.1 Pa is not valid for the Japanese design using pebbles of about 1 mm diameter. In this case, the thermal gradient through the Li_2O layer is much less important, and the tritium pressure in the sweeping gas should go down to 0.03 torr, while the sweeping gas flow rate decreases to 200 $m^3 \cdot h^{-1}$. This allows the tritium inventory in the blanket reprocessing system to decrease about one order of magnitude.

5.4. Waste processing system

One of the INTOR requirements is to keep the tritium release at a level as low as reasonable. This implies reprocessing of all gaseous wastes coming from the plasma vacuum vessel, from the blanket system, from the neutral-beam lines and from the gas feed bottles. This reprocessing is performed by the waste processing system.

TABLE VIII-23. ESTIMATE OF WASTE COMPOSITION

Origin	Composition	Flow rate
Primary coolant electrolysis cell tank	O_2, KOT, KOH, H_2O	0.043 $m^3 \cdot h^{-1}$
Neutral injectors and torus feed cold traps	O_2, N_2	not estimated
Plasma exhaust cold traps	D_2O, T_2O, HTO, O_2, N_2, CO, CO_2, CT_2D_2, NDT_2, NTD_2	not estimated
Breeding tritium cold traps	T_2O, He	0.024 $m^3 \cdot h^{-1}$

The basic assumption of the process to be discussed hereafter is that the concentration of organic compounds such as methane, a result of the use of graphite in the torus, is not excessively high in the wastes. One possible process is the following:

Impurities are driven on a uranium bed heated up to a temperature level higher than 600°C, where compounds like water, methane, ammonia etc. are decomposed by chemical reactions with metallic uranium, giving uranium compounds and free hydrogen that diffuses through a palladium-silver membrane. This hydrogen is pumped through the membrane and directed to the purification of the plasma exhaust processing system. This process works as long as the hydrogen partial pressure in front of the membrane is higher than that at the back, after which the process stops. It is possible to decrease this pressure to a lower value by using a bed of pyrophoric uranium, where hydrogen is trapped as UH_3. When the tritium content in the waste is low enough and the uranium bed does not react either, gaseous wastes are directed to the stack, after a final oxidation and water extraction.

The waste composition is roughly estimated in Table VIII-23, impurities coming from plasma or primary coolant being unknown up to date.

5.5. Tritium inventory

A first estimation of the tritium inventory is carried out by taking into account all the processing lines of the tritium system which have been described above. For this preliminary inventory, different assumptions have been put forward:

- The tritium hold-up of catalytic beds is approximately 1 to 10% of the tritium flow per hour;
- The gas tank hold-up is calculated for a retention time of 10 min.

A few numerical values of the INTOR Phase One are taken into account in the following detailed calculations (see Table VIII-24):

- vacuum pumps 120 g
- pellet fabrication[1] 200 g
- isotopic separation system 120 g
- tritium bottle from external supply (each) 10 g

The preliminary results are presented in Table VIII-25.

5.6. Atmosphere processing system

The tritium handling system has to process contaminated atmospheres to avoid any accidental or routine tritium leaks. To protect workers against radioactivity, a secondary containment, consisting of glove-boxes and 'caissons', is absolutely necessary. This secondary containment is ventilated by argon for minimizing the tritiated water formation in these atmospheres as far as possible. The tertiary containment, consisting of the tritium room itself, the reactor hall and the hot cells, minimizes any tritium release to the environment. A description of these systems is given in Section 3.

5.7. Conclusions

As presented here, the INTOR tritium system may induce wrong conclusions with regard to the tritium technology development. A large number of optimistic assumptions were made during the studies, and these assumptions must be confirmed through extended experimental programmes, complemented by industrial development.

Some of these problems arise at the interface of the tritium system with the tokamak itself. As an illustration, valves separating the INTOR vacuum chamber and cryopumps do not exist. Valves of large dimensions (diameter = 160 cm), ultra-high-vacuum-tight, tritium-compatible and, if possible, with a very short closure time, have to be developed.

In the tritium system itself, the cold trapping of impurities must be studied experimentally. The same situation prevails for the cold trapping of water vapour in the blanket reprocessing line or in the atmosphere detritiation systems.

[1] The possibility of decreasing this figure looks reasonable.

TABLE VIII-24. TRITIUM SYSTEMS INVENTORY

Plasma exhaust and neutral injectors:	
cryopumps (12) (2 hours)	120 g
gas storage units (12) (2 hours)	120 g
liquid storage before isotopic separation	10 g
cryodistillation	120 g
	370 g
Breeding tritium (solid):	
gas storage tanks (12) (10 min)	0.35 g
catalytic beds	0.42 g
liquid nitrogen cold trap (7 days) (lower flow rate/regeneration time should decrease this figure)	350.00 g
liquid nitrogen cold trap hold-up	38.00 g
ion exchange resin	7.00 g
liquid storage tank before electrolysis (7 days) (same as above)	350.00 g
gas tank (10 min)	0.35 g
	746.00 g
Neutral injectors and torus feed:	
T_2 gas storage tank (10 min)	11 g
DT gas storage tank (10 min)	5 g
tritium bottles (3)	30 g
pellet injectors	200 g
	246 g
Primary coolant detritiation:	
hydrogen cryodistillation column	60 g
primary coolant processing	5 g
	65 g

TABLE VIII-25. TOTAL TRITIUM INVENTORY (SOLID BREEDER)

Plasma exhaust and neutral injectors	370 g
Breeding tritium	746 g
Primary coolant detritiation	65 g
Wastes	not estimated
Atmosphere	1 g
Neutral injectors and torus feed	245 g
	1427 g
Storage	2300 g
Breeding blanket	500 – 1000 g
First wall	100 – 1000 g
Total	4330 – 5730 g

An electrolytic cell, able to process tritiated water with a high tritium content, must be carefully designed and experimented in mock-up situations and then with tritium itself. The efficiency of the waste reprocessing line mainly depends on the chemical nature of the impurities; if large quantities of organic compounds have to be reprocessed (this situation could arise if graphite is used in the machine), their chemical decomposition on uranium beds may be a concern, etc.

So the process presented in this paper will provide a workable solution only if the experimental programme is running through without too severe problems.

One important remark concerning the tritium inventory is that the fraction contained in the blanket reprocessing system may be very high, depending on the helium flow rate. An optimization of tritium inventory in-blanket and in the reprocessing system has to be performed.

The total tritium inventory is estimated to be of the order of 4 to 6 kg (Table VIII-25).

6. SAFETY CONSIDERATIONS

6.1. Accident analysis

Since design details of relevant tritium system components are not available, an accident analysis of these systems should be considered to be very preliminary.

TABLE VIII-26. VULNERABLE AND NON-VULNERABLE TRITIUM INVENTORIES (IN GRAMS)

I. Vulnerable inventories		
(a) In reactor building		
Plasma chamber	0.08	
Limiter/divertor/first-wall coolant	3	
Blanket coolant: solid breeder	0.006	
liquid breeder	2	
Shield coolant	0.006	
Cryopumps	120	12 units
Fuellers	20	2 units
Subtotal	145	
(b) In tritium system boxes		
Blanket tritium recovery system (solid breeder)	up to 746	350 g in liquid nitrogen cold trap, 350 g in liquid storage bank, 38 g in another cold trap, 17 g in ion exchange resins
Fuel gas reprocessing system	up to 250	120 g in cryodistillation unit, 120 g in gas storage tanks, 10 g in liquid storage unit
Pellet preparation system	up to 200	
Primary coolant detritiation unit	up to 65	
Others	21	
Subtotal	1282	
Subtotal vulnerable inventories	1427	
II. Non-vulnerable inventories		
(a) In reactor building		
Blanket: solid breeder	500–1000	divided in 600 tubes or 72 modules
liquid breeder	200	
first-wall/limiter/divertor	100–1000	
Blanket recovery lines	up to 3	
Subtotal	600–2000	

TABLE VIII-26 (cont.)

(b) In tritium system boxes	
Storage	2300
Subtotal non-vulnerable inventories	2900–4300
Total	4330–5730

The potential tritium releases in accident situations are determined by tritium inventories being in vulnerable form in reaction systems and components.

The list of tritium inventories is given in Table VIII-26.

The potential tritium releases in different accident situations are shown in Table VIII-27.

6.2. INTOR radiation impact on population

The radiation environment near the INTOR installation will be essentially controlled by gas and aerosol releases of tritium. The contribution of other radioactive sources can be considered to be negligible [2].

Up to 20 Ci per day tritium stack release is arbitrarily assumed during normal operation, while accidentally up to 10^5 Ci can be released.

The radiation impact on population due to gas and aerosol releases of a radionuclide depends on the near-ground concentration. Knowing this concentration, one can estimate the dose equivalent, using the dose factors which take into account various paths of the radionuclide impact on the human organism.

The calculation technique developed by Pasquill [6] for obtaining the near-ground tritium concentration has been applied. Average European meteorological data were used. The assumed values of the calculation parameters are given in Table VIII-28.

Calculations have been carried out for a 1-m-diam. stack assuming an effluent-gas temperature of 25°C. H = 0, 20, 60, 100 m were considered. The first two cases imitate releases from the INTOR building (e.g. when the containment is damaged), the last two correspond to releases from a stack of varying height.

The results for normal operation are presented in Fig. VIII-33. The concentration values are normalized to the release rate of 1 Ci per day.

The radius of the sanitary protective zone (the plant site), where no inhabitants are permitted, is arbitrarily assumed to be 1 km. At this distance, the dose rates

TABLE VIII-27. POTENTIAL TRITIUM RELEASES IN ACCIDENT SITUATIONS

1. Rupture of the plasma chamber vessel	Just after the rupture air flows into the plasma chamber. When the pressure in the plasma chamber and in the reactor room reach equilibrium, tritium is released through thermal expansion and natural convection. The amount of tritium released may be up to a tritium quantity in the plasma vacuum chamber of 0.08 g. In the case of accident cyropumps should be cut off and tritium release from them must be prevented.
2. Rupture of the first-wall coolant pipe	Up to 2t of cooling water can flow into the plasma chamber. The pressure in the chamber rises to 0.5 MPa, and the chamber vessel can be breached. The tritium release can be, at most, the sum of tritium inventories in the plasma chamber (0.08 g), in 2t of the water cooling the first wall (<0.02 g), and outgoing for the first wall (≈0.1–0.2 g). It is assumed that cryopumps are cut off and tritium release from them is prevented.
3. Accident of a cryopump unit (e.g. due to hydrogen detonation)	Release of, at most, 10 g of tritium to reactor room
4. Rupture of a cryopump gate valve during regeneration.	Release of, at most, 10 g of tritium to plasma chamber or in the reactor hall.
5. Rupture of the distillation columns and surrounding vacuum jacket in the isotope separation unit of the fuel gas reprocessing system (e.g. because of loss of refrigeration)	Release of, at most, 120 g of tritium into glove-box of ≈20 m^3 with subsequent removal through inert gas purification system
6. Rupture of components of the blanket tritium recovery system (liquid nitrogen cold trap, liquid storage tank, electrolysis unit)	Up to 350 g of tritium in tritiated water can escape into the glove-box. If glove ports are not plugged and the temperature of glove-box is 25°C, tritium release rate to the tritium processing room can be up to 10^3 Ci·h^{-1}.
7. Rupture of blanket vessel	Huge tritium releases due to blanket accidents are not expected, since in the case of solid blanket tritium is retained by the solid breeder and since breeding material is allocated in many tubes or modules. An accident involving

TABLE VIII-27 (cont.)

	all the numerous blanket modules is highly unlikely. In blanket-in-tubes design version accidental tritium release can be up to 2 g. In high-temperature blanket-out-of-tubes design version with 72 blanket modules it is expected to be up to 4 g and, on the assumption that the total tritium inventory in the blanket is 500–1000 g, it is expected to be up to 7–14 g. In liquid eutectic $Li_{17}Pb_{83}$ blanket, tritium inventory is, at least, one order of magnitude lower than in solid breeder.
8. Rupture of coolant pipes in the blanket	Cooling water flows into the blanket and reacts with Li_2O. Heat generation rate can be about 2 kW at water leak of 0.3 $kg \cdot s^{-1}$. Temperature in the blanket rises and pressure in the blanket vessel can exceed the allowable one of 0.1 MPa. The blanket vessel ruptures, pressure in the plasma chamber may increase and rupture of the plasma chamber vessel can occur. Release into the reactor room of, at most, the sum of tritium inventories in the corresponding part of blanket module (14 g), plasma chamber (0.08 g) and blanket cooling system (0.006 g). For the $Li_{17}Pb_{83}$ blanket, a pipe break inside the vessel may cause pressure oscillations with a peak of about 9 MPa and a static final pressure equal to the coolant pressure (6.5 MPa) after about 5 ms. Under these circumstances, the stresses on the structure are very high, particularly on the flat vessel walls. Therefore, ribs uniformly distributed across the blanket unit to increase the overall stiffness of the structure are provided. In case of blanket unit rupture, 0.3 g of tritium are released.
9. Rupture of coolant pipes in the shield	Maximum tritium release is 0.06 g.

TABLE VIII-27 (cont.)

10. Accident in tritium storage system	Tritium storage (about 2.3 kg) is subdivided into small units of maximum tritium inventory equal to 10 g. Two kinds of storage may be contemplated: gaseous form in small vessels or hydride form on getter beds. In both cases, measures have to be taken to prevent that an accident may involve more than one unit.

TABLE VIII-28. ASSUMED VALUES OF CALCULATION PARAMETERS

Average wind speed with respect to Pasquill's categories, $m \cdot s^{-1}$					
A	B	C	D	E	F
2.5	3.4	2.6	4.5	2.7	2.0
Pasquill's category frequencies					
A	B	C	D	E	F
0.026	0.114	0.230	0.322	0.178	0.130

are 9.6, 5.5, 1.3, 0.5 mrem per year for H = 0, 20, 60, 100 m, respectively. For these estimates a dose factor value of 1.6×10^{-3} (mrem per year)/(pCi·m^{-3}) [6] has been used.

According to the accepted INTOR concept of reducing the routine releases to values as low as reasonably achievable (ALARA), the goal dose commitment at the site boundary should not exceed 5 mrem per year [2]. The calculation results show that such a condition can be fulfilled by applying a stack of moderate height ($H \approx 40$ m).

Similar calculations have been performed for a 10^5 Ci accidental release of tritium (10 g). The results are given in Fig. VIII-34. The dose values at the site boundary are 1.1, 0.47, 4.6×10^{-2}, 2.4×10^{-2} rem for H = 0, 20, 60, 100 m, respectively.

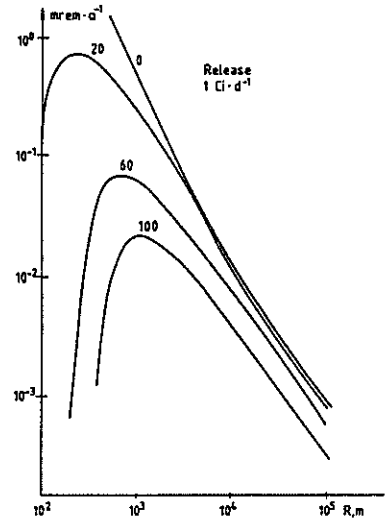

FIG. VIII-33. Dose rates at various release heights versus distance.

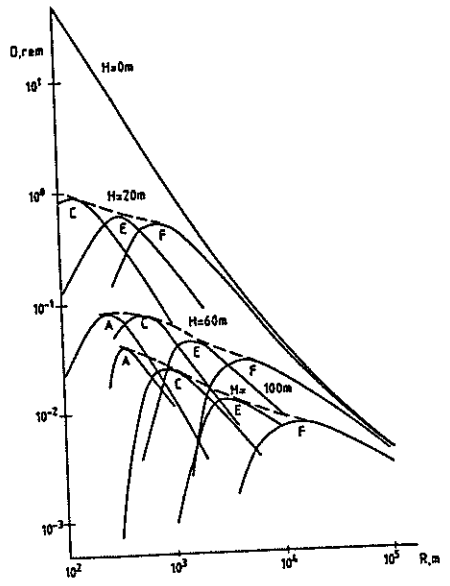

FIG. VIII-34. Maximum dose versus distance at 10^5 Ci accidental release of tritium.

Figure VIII-35 shows the dose values depending on the distance from the release point both for normal INTOR operation and for accidental release. Release heights of 60 and 0 m have been assumed.

It is obvious that the dose equivalent at the site boundary, even if it does not exceed the permissible limit, does not provide a complete characteristic of the radiation impact on population. According to the currently used concept of thresholdless linear dependence of low-dose radiation impact on large groups of population, one should take into consideration the possibility for both somatico-stochastic and genetic effects to appear (usually cancer frequency and genetic damages are meant).

As a measure of low-dose impact on large groups of population, the population dose is used, expressed in man-rem.

To evaluate it, not only information on radiological environment, but also data on the population distribution are needed. Let us assume that, within a radius of 80 km around the INTOR, 10^6 people are living [2] and the distribution of population is uniform. It is seen from Fig.VIII-35 that, at a distance of 20 km, the dose rate due to routine releases becomes lower than 0.1% of the natural background (the latter average value is 100 mrem per year). It is impossible, at

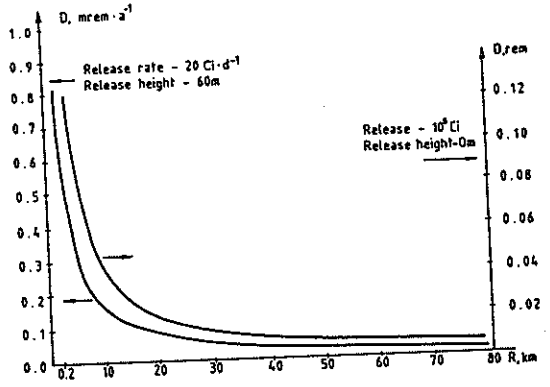

FIG. VIII-35. Dose rate versus distance from release point.

this distance, to reveal the INTOR tritium release contribution to the population dose. In such a case, the population dose for population within 20 km will be 12 man·rem per year.

During an accidental release of 10^5 Ci, the dose equivalent to individuals at a distance of 80 km will be about 6 mrem (one order of magnitude within the natural background fluctuations [22, 23]). The population dose due to an accidental release within this 80 km range is 8×10^3 man·rem.

According to the ICRP publications Nos 26 and 27, the risk of a death due to cancer and genetic damage in large groups of population exposed to radiation is 1.65×10^{-4} (man·rem)$^{-1}$. Consequently, the risk to the mentioned population group (10^6 people) will be 3×10^{-2} per 15 years of INTOR normal operation and 1.3 per accident. Thus the INTOR radiation impact both due to routine and accidental releases does not result in an actual risk to the entire exposed population group. The value of the death risk due to cancer to an individual, averaged over the entire world population, is about $(1-1.5) \times 10^{-3}$ per year [24]. The corresponding risk levels from INTOR will be 2×10^{-9} per year at routine tritium releases and 1.3×10^{-6} at an accident which is negligibly small.

REFERENCES TO CHAPTER VIII

[1] INTOR Group, International Tokamak Reactor: Zero Phase (Rep. Int. Tokamak Reactor Workshop Vienna, 1979), International Atomic Energy Agency, Vienna (1980); see also Summary in Nucl. Fusion 20 (1980) 349.

[2] INTOR Group, International Tokamak Reactor: Phase One (Rep. Int. Tokamak Reactor Workshop, 1980–81), International Atomic Energy Agency (1982); see also Summary in Nucl. Fusion 22 (1982) 135.

[3] European Community Contributions to the INTOR Phase-Two-A Workshop, Rep. Commission of the European Communities, Brussels (1982).

[4] Japan Contribution to the INTOR Phase-Two-A Workshop, Rep. Japan Atomic Energy Research Institute, Tokai-mura (1982).

[5] USA Contribution to the INTOR Phase-Two-A Workshop, Rep. FED-INTOR/82-1, Georgia Institute of Technology, Atlanta (1982).

[6] USSR Contribution to the INTOR Phase-Two-A Workshop, Rep. Kurchatov Institute, Moscow (1982).

[7] WIENHOLD, P., PROFANT, M., WAELBROECK, F., WINTER, J., J. Nucl. Mater., 93 & 94 (1980) 866.

[8] BASKES, M.I., J. Nucl. Mater. 92 (1980) 318.

[9] GONZALEZ, O.D., ORIANI, R.A., Trans. Metall. Soc. 233 (1965) 1882.

[10] SAWATZKY, A., J. Nucl. Mater. 2 (1960) 321.

[11] GORODETSKY, A.E., ZAKHAROV, A.P., SHARAPOV, V.W., ALIMOV, V.Kh., J. Nucl. Mater. 93 & 94 (1980) 588.

[12] TANABE, T., SAITO, N., ETOH, Y., IMOTO, S., J. Nucl. Mater. 103 & 104 (1981) 483.

[13] JONES, P.M.S., GIBSON, W.R., J. Nucl. Mater. 21 (1967) 353.

[14] SWANSIGER, W.A., BASTASZ, R., Proc. Tritium Tech. in Fission, Fusion and Isotopic Appl., ANS (1980) 91.

[15] MIYAKE, M., et al., J. Nucl, Mater. 103 & 104 (1981) 477.

[16] PIERINI, G., POLCARO, A.M., RICCI, P.F., VIOLA, A., Tritium Recovery from Liquid $Li_{17}Pb_{83}$, presented at 12th SOFT, Jülich (Sept. 1982).

[17] VELECKIS, E., personal communication to N. Hoffman, ETEC (June 1981).

[18] REITER, F., ROTA, R., CAMPOSILVAN, J., Thermodynamic Properties of $Li_{17}Pb_{83}$, 12 th SOFT, Jülich (Sept. 1982).

[19] WU, C.H., BLAIR, A.J., A Study of the Interaction of Tritium with Liquid $Li_{17}Pb_{83}$, 12th SOFT, Jülich (Sept. 1982).

[20] COEN, V., FENICI, P., KOLBE, H., ORECCHIA, L., SASAKI, T., Compatibility of AISI 316 L Stainless Steel with $Li_{17}Pb_{83}$ Eutectic , J. Nucl. Mater. 110 (1982) 114.

[21] TORTORELLI, R.F., et al., Corrosion and Compatibility Considerations of Liquid Metals for Fusion Reactors, Proc. 2nd Top. Meeting on Fusion Reactor Materials, Seattle, Wa. (1981).

[22] BOCHVAR, I.A., et al., Measurements of the USSR Towns Population Exposure to the Background Radiation in 1964–1965, At. Ehnerg. 22 (1967) 59.

[23] PERTSOV, L.A., Ionizing Radiation of the Biosphere, Moscow, Atomizdat (1973).

[24] SERENKO, A.F., ROMENSKY, A.A., Eds, Zabolevayemost' naseleniya SSSR zlokachest-vennymi novoobrazovaniyami i smertnost' ot nikh. (Cancer Morbidity and Corresponding Mortality of the USSR Population), Moscow, Meditsina (1970).

[25] ABDOU, M., et al., Tritium FED/INTOR/TRIT/81-01, USA Input to INTOR Workshop Session III, Phase-Two-A (December 1981).

[26] ABDOU, M., et al., Tritium and Safety, FED-INTOR/TRIT/82-4, USA Input to te the INTOR Workshop, Session V, Phase-Two-A (July 1982).